

2022

# Forest Risk Map

Mapping des Risikos von Waldbeständen  
im Klimawandel

Final Report



# **Forest Risk Map with Focus on Central and Eastern European Coniferous Forests**

## **BFW**

Silvio Schüler  
Carina Heiling  
Thomas Gschwantner  
Ambros Berger  
Katrín Windisch-Ettenauer

## **ZAMG**

Matthias Schlögl  
Katharina Enigl  
Christoph Matulla

## **Mondi AG**

Leo Arpa  
Dietmar Hagauer

**BFW - Bundesforschungs- und Ausbildungszentrum für Wald, Naturgefahren und Landschaft**  
Seckendorff-Gudent-Weg 8  
1131 Wien

and

**ZAMG Zentralanstalt für Meteorologie und Geodynamik**  
Hohe Warte 38  
1190 Wien

and

**Mondi AG**  
Marxergasse 4A 1030 Wien

## 1 Content

<b>1</b>	<b>CONTENT</b> .....	<b>1</b>
<b>2</b>	<b>BACKGROUND AND OBJECTIVES</b> .....	<b>2</b>
<b>3</b>	<b>DATA/METHODS</b> .....	<b>2</b>
3.1	CLIMATE CHANGE SCENARIOS .....	2
3.1.1	<i>RCP-scenarios</i> .....	3
3.1.2	<i>SSP-scenarios</i> .....	3
3.2	FOREST STOCKS .....	3
3.2.1	<i>Growing stock in Austria</i> .....	3
3.2.2	<i>Growing stock in Europe</i> .....	4
3.2.3	<i>Uncertainties</i> .....	5
3.3	TREE SPECIES DISTRIBUTIONS TODAY AND FUTURE .....	5
3.4	CLIMATE AND WEATHER RISKS .....	6
3.4.1	<i>Forest damage</i> .....	6
3.4.2	<i>Identification of similar climatological regions based on 19 bioclimatic variables</i> .....	8
3.4.3	<i>Identification of similar climatological regions based on the ECLIPS2.0 dataset</i> .....	9
3.5	RISK MAP CALCULATION .....	13
<b>4</b>	<b>RESULTS</b> .....	<b>18</b>
4.1	CURRENT FOREST STOCKS .....	18
4.1.1	<i>Growing stock in Austria</i> .....	18
4.1.2	<i>Growing stock in Europe</i> .....	19
4.1.3	<i>Uncertainty</i> .....	21
4.2	CLIMATE AND WEATHER RISKS .....	22
4.2.1	<i>Damage models</i> .....	22
4.2.2	<i>Identification of similar climatological regions based on Bioclim</i> .....	24
4.2.2.1	2021 - 2040 .....	24
4.2.2.2	2041 - 2060 .....	25
4.2.2.3	2061 – 2080 .....	25
4.2.2.4	2081 – 2100 .....	26
4.2.2.5	Discussion .....	26
4.2.3	<i>Identification of similar climatological regions based on ECLIPS2.0</i> .....	27
4.2.3.1	RCP4.5 .....	27
4.2.3.2	RCP8.5 .....	28
4.2.3.3	Discussion .....	28
4.3	RISK ANALYSIS .....	29
4.3.1	<i>Definition of risk measures and stock changes</i> .....	29
4.3.2	<i>Risk Maps</i> .....	30
4.3.3	<i>Current and potential future stocks</i> .....	33
4.3.4	<i>Stock changes</i> .....	36
<b>5</b>	<b>CONCLUSION</b> .....	<b>40</b>
<b>6</b>	<b>REFERENCES</b> .....	<b>45</b>

## 2 Background and Objectives

Large-scale disturbances in forests of Central, Eastern, and Southeastern Europe represent a growing operational risk for forestry and the wood-processing industry (paper, panel, and sawmill industries). The most important causes of large-scale calamities are weather extremes: droughts (whose significant increase seems to show a close coupling to the increasingly unfolding climate change), heavy storm and wet snow events, and ice breakage. As a consequence of these climate change-related extreme events and the time-consuming processing of damaged wood, more breeding material for bark-dwelling bark accumulates. Moreover, the longer growing season and higher temperatures also enable bark beetles to reproduce faster allowing more breeding generations per season. Together with the reduced tree vigor, this leads to increases in insect pest populations, the consequences of which far exceed the extent of the primary damage.

In the short term, large-scale calamities lead to an oversupply of damaged wood and strong price fluctuations on the timber market. For forest managers, this means higher costs, which are due to the processing of increased volumes of damaged wood and the associated investments for the implementation of far-reaching measures (ensuring work safety). For the wood processing industry, these developments might be accompanied by a reduction of the available wood assortments in the medium term and higher costs for logistics and storage. In the long term, however, not only reductions in the variety of the wood assortment is endangered, but even the availability of the raw material wood for the supply of the wood-processing industries might be at risk.

Regional risk for large-scale climate change-induced disturbances is influenced by several factors. These include (1) the likelihood of the occurrence of extreme weather conditions, particularly spring and summer droughts, and events such as storms, wet snow, and ice breakup, if applicable; (2) the current occurrence of spruce and pine, the coniferous tree species most at risk in Central Europe; (3) the wood or biomass supply of these tree species as a potential extent of damage; and (4) the long-term suitability of these tree species in the particular region.

For some of these factors, scientific knowledge already exists. For example, numerous publications exist at the European level on the occurrence of the most important tree species under present climate (Mauri et al. 2017) and the expected future climate (Schueler et al. 2014, Dydersky et al. 2018), on wood and biomass supply in European forests (Alberdi et al. 2020, Vauhkonen et al. 2019), and on the risk of extreme climatic events (Ledermann et al. 2010, Pasztor et al. 2014, 2015, Matulla et al. 2008, Haslinger et al. 2016). However, these individual results have never been combined and used for a comprehensive risk analysis before. In the present project, these risks are to be combined for the first time in cooperation between forest scientists and climate researchers in order to provide a reliable planning basis for the pulp and paper industry.

## 3 Data/Methods

### 3.1 Climate change scenarios

One of the most relevant tasks of climate research is the assessment of climate impacts based on the development of future climate in the face of increasing greenhouse gas concentration. Future emissions of anthropogenic greenhouse gases depend on various economic, social, and political developments that are fundamentally unpredictable. Since the actual future development is inherently uncertain, climate research has to rely on a wide range of assumptions about future human development. Based on these assumptions a diverse range of emissions scenarios is established, that in turn forms the basis for projections of future climate development.

Different generations of such greenhouse gas scenarios exist. The first set of scenarios were the IPCC scenarios from 1992, called IS92 scenarios. They were replaced in 2000 by the so-called SRES scenarios (named after the *Special Report on Emissions Scenarios*). The SRES scenarios specifically took possible developments in the areas of population growth, economic and social development, technological



changes, resource consumption and environmental management throughout the 21st century into account. These climate scenarios, divided into “scenario families” (A1, B1, A2, and B2) were the basis for both the IPCC’s 3<sup>rd</sup> Report of 2001 and the 4<sup>th</sup> Report of 2007. For the 5th report of 2013 a new type of scenarios was developed, namely the so-called *Representative Concentration Pathways* (RCPs). As opposed to the SRES scenarios, the RCP scenarios did not derive the radiative forcing of increasing greenhouse gas concentrations from socio-economic factors, but simply specified certain change in radiative forcing by 2100 relative to pre-industrial forcing. In total, four pathways have been suggested, each of them describing different climate futures, which are considered possible depending on the volume of greenhouse gases emitted in the coming decades. The RCPs – originally RCP2.6, RCP4.5, RCP6, and RCP8.5 – are labelled after a possible range of radiative forcing values in the year 2100 (2.6, 4.5, 6, and 8.5 W/m<sup>2</sup>, respectively). For example, RCP6.0 represents an additional radiative forcing from anthropogenic greenhouse gases of 6.0 W/m<sup>2</sup> in 2100 relative to 1850.

Recently, the economic and social justification for the RCP scenarios has been provided by the so-called *Shared Socioeconomic Pathways* (SSP). Unlike the RCP scenarios and similar to the older SRES scenarios, SSP scenarios focus on global societal, demographic and economic changes and are already included in the latest model generation CMIP6 (Coupled Model Intercomparison Project Phase 6), which was used for the IPCC’s 6<sup>th</sup> Assessment Report (2021). In fact, SSP scenarios complement RCP scenarios with socio-economic factors.

### 3.1.1 RCP-scenarios

For the present study, the two Representative Concentration Pathways scenarios RCP4.5 and RCP8.5 were selected. These scenarios stand for climate change between the period of 1971-2000 until 2071-2100 in the range of +1.4 - 4.2°C for RCP4.5 and + 2.7 – 6.0°C for RCP8.5 across Europe (Jacob et al. 2004).

### 3.1.2 SSP-scenarios

The SSP scenarios are composed of two major components, with the so-called baseline scenarios (SSP1 - SSP5) representing socioeconomic, demographic, political, technological, and institutional developments.

- SSP1: Sustainability
- SSP2: Middle of the road
- SSP3: Regional rivalry
- SSP4: Inequality
- SSP5: Fossil-fueled development

SSP scenarios show for the different pathways how emissions could develop without climate regulations (Riahi et al., 2017). By comparing the results of a scenario analysis with and without climate action, the effectiveness of climate action can be evaluated. The second component is the so-called Representative Concentration Pathways (RCPs; van Vuuren et al., 2011), which represent emission pathways and their impact on radiative forcing (GSFC Germany, 2019).

## 3.2 Forest Stocks

The evaluation of potential forest damage risks requires information about the current growing stocks of forests. In the present study we focus geographically on the one hand on Austria, and on the other hand on the growing stock distribution in other European countries.

### 3.2.1 Growing stock in Austria

For Austria comprehensive statistics about the forest resources are available through the periodical sample-based assessments by the Austrian National Forest Inventory (NFI). The Austrian NFI estimates growing stocks at three different regional levels, the country-level, the level of federal states (which correspond to NUTS2 regions), and the level of forest service districts (Bezirksforstinspektionen, BFIs). In this project we applied the highest spatial resolution of BFIs. Growing stocks were calculated in terms of stemwood volume (m<sup>3</sup>) and above-ground biomass (t) for the latest complete NFI (2007/09). To present the results, first the total growing stock including all tree species is mapped according to BFI, then a distinction is made between conifers and deciduous trees, and within the conifers the focal tree species Norway spruce and Scots pine are distinguished, and within the deciduous trees the European beech is

distinguished. The maps represent growing stocks in terms of stem volume and above-ground biomass (AGB) per ha of BFI area ( $\text{m}^3/\text{ha}$  and  $\text{t}/\text{ha}$ ). The same presentation scheme is used for other European countries for NUTS2 regions, as described in the subsequent section.

### 3.2.2 Growing stock in Europe

For other European countries, less detailed information on growing stocks was commonly available. Nevertheless, several studies and statistics were published in the recent years that allow for the estimation of wood resources also for other European countries. A review, analysis, and synthesis of available data sources was conducted for estimating the growing stock in countries at the European level. The review included international statistics and published maps. The compiled international forest statistics include the reports of the

- Forest Resources Assessment 2020
- Forest Europe 2020
- UNECE/FAO timber section 2017-2019

From these sources primarily the growing stock information from the countries is relevant, although further information such as forest area, above-ground biomass, or removals may be used during the analysis. The review of available maps on forest resources in Europe revealed several sources of potential interest for the analyses (Table 1).

**Table 1: Available map information on forest resources.**

Source	Information	Reference year	Coverage	Grid cell size	Reference system	Data format	Technology
Thurner et al. 2014.	AGB C ( $\text{kg}/\text{m}^2$ ), uncertainty	2010	northern hemisphere	0,01°	WGS84	?	data from Santoro et al. 2011
Santoro 2018.	Growing stock volume ( $\text{m}^3/\text{ha}$ ), uncertainty (SE)	2010	global	0,0009° ~ 100 m	WGS84	.tif	SAR, optical sensor, LIDAR, auxiliary data
	AGB ( $\text{t}/\text{ha}$ ), uncertainty (SE)						
Spawn et al. 2020.	ABG Carbon ( $\text{Mg C}/\text{ha}$ ), uncertainty	2010	global	0,0028° ~ 300 m	?	.tif	data from Santoro et al. 2018
	BGB Carbon ( $\text{Mg C}/\text{ha}$ ), uncertainty						
Verkerk et al. 2019.	Total biomass availability ( $\text{Tg C}/\text{year}$ )	2020	Europe	10 x 10 km	ETRS-LAEA	.tif	EFISCEN Scenario analyses (BASE Szenario)
	Relative biomass availability ( $\text{t}/\text{ha}/\text{year}$ )						
Mauri et al. 2017.	Tree species occurrence	etwa 2000 - 2010	Europe	1 x 1 km	ETRS89-LAEA	.csv, point shapefiles	merged from Forest Focus, Biosoil, NFIs
Bruce et al. 2011.	Tree species occurrence	etwa 2000 - 2010	Europe	1 x 1 km	ETRS-LAEA	.tif	ICP, NFIs, EFISCEN, FRA, ECE/FAO

After examination of these data sets, Santoro (2018) and Bruce et al. (2011) were found to be most suitable for further analyses. Figure 1 displays these two data sources.

The collected data sources were processed and analysed in the GIS environment to obtain growing stock maps by tree species at European level. For this purpose, from tree species data (Bruce et al. 2011) tree group rasters were derived by summarising rasters for coniferous and deciduous species. These rasters express the share of a tree species per pixel. Next, both datasets (Bruce et al. 2011, Santoro 2018) were set to the same coordinate reference system (WGS84), were resampled to the same spatial resolution (1x1km), and were finally aggregated to the NUTS2-level. In line with the results for Austria, growing stock information including all tree species was obtained, then distinguished between conifers and broadleaves, and further distinguished into Norway spruce, Scots pine, and European beech. At the European level growing stock was calculated for NUTS2 regions. As previously mentioned, growing stock data are also available at country-level (NUTS0) from international statistics, most recently published in the Global Forest Resources Assessment 2020 (FAO 2020). This information implies several advantages as it represents up-to-date information, is frequently based on terrestrial NFI data, applies a common set of definitions, and represents country-level conditions. Therefore, country-level growing stock volume and AGB from FRA 2020 were used as basic data and the distribution within countries on NUTS2 level was

obtained from Santoro (2018) for growing stock and Bruce et al. (2011) for species distribution, because this information is not contained in the FRA 2020 data.

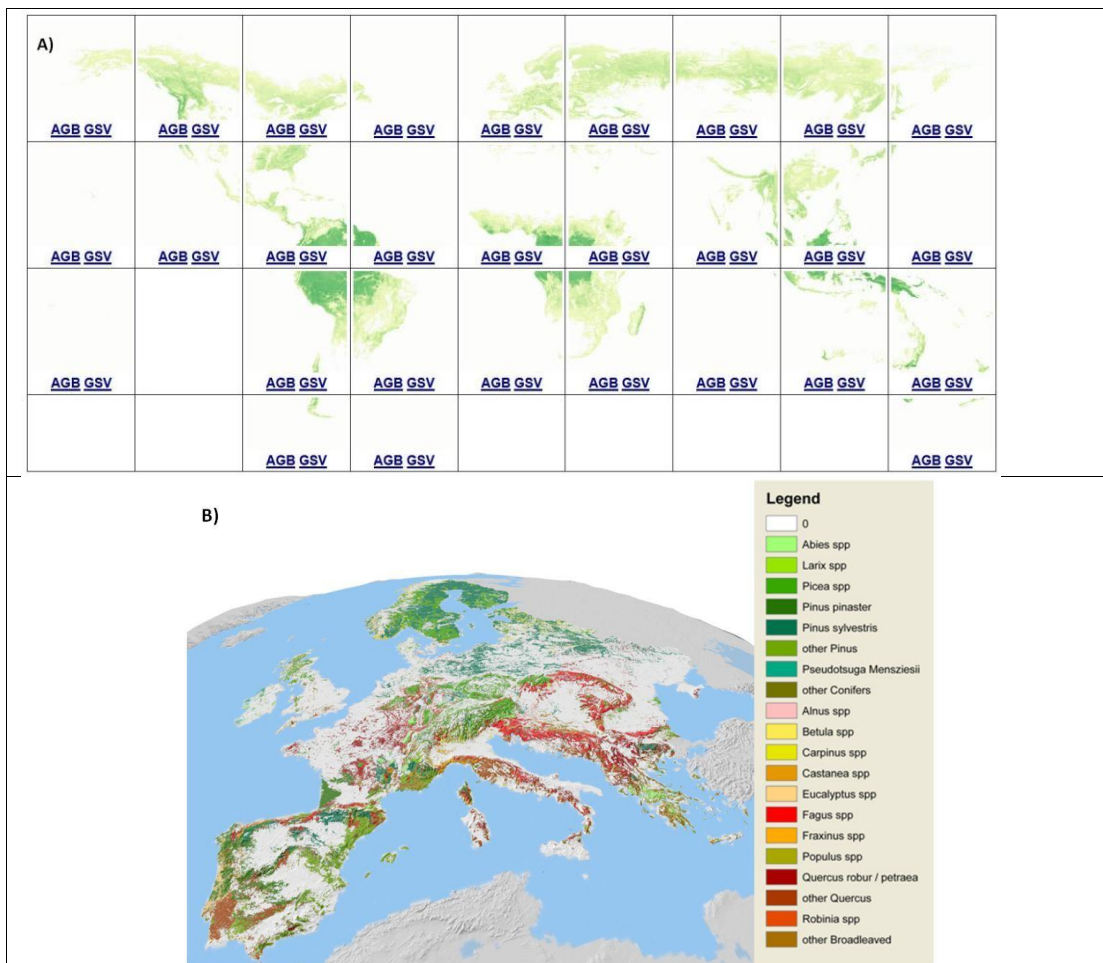


Figure 1: Data sets for deriving growing stock estimates: A) Santoro (2018), B) Bruce et al. (2011).

### 3.2.3 Uncertainties

Growing stock results from the Santoro (2018) and Bruce et al. (2011) datasets were obtained also for Austria where corresponding results from the Austrian NFI 2007-2009 are available. In order to obtain information about the involved uncertainties, the growing stock estimates were compared for Austrian NUTS2 regions. It turned out that Santoro (2018) overestimated the growing stock for some regions, which is most likely due to the thinly stocked shrub forest in high mountain locations and inaccessible forest which is not surveyed by the Austrian NFI.

Furthermore, the results from the Santoro (2018) and Bruce et al. (2011) datasets were compared to the growing stock results from FRA 2020 at country-level to identify deviations from the data provided in international statistics. For some countries, the stocks matched well, whereas in other countries the deviations were substantial. Santoro et al. (2018) state that the uncertainty of their estimates can go as high as 40 % on the small scale. All this led to the above-mentioned decision to use the FRA 2020 data as basis.

### 3.3 Tree species distributions today and future

Ecological niche models have been the most widely used tools to estimate the potential climatic suitability of species worldwide. The reliability of such estimations depends on the model algorithm and the input data such as climate and species occurrence. We used a dataset of the potential distribution of seven ecologically and economically important tree species of Europe in terms of their climatic suitability

with an ensemble approach while accounting for uncertainty due to model algorithms. The distribution models (Chakraborty et al. 2021) were used as the basis for the follow-up risk-analysis.

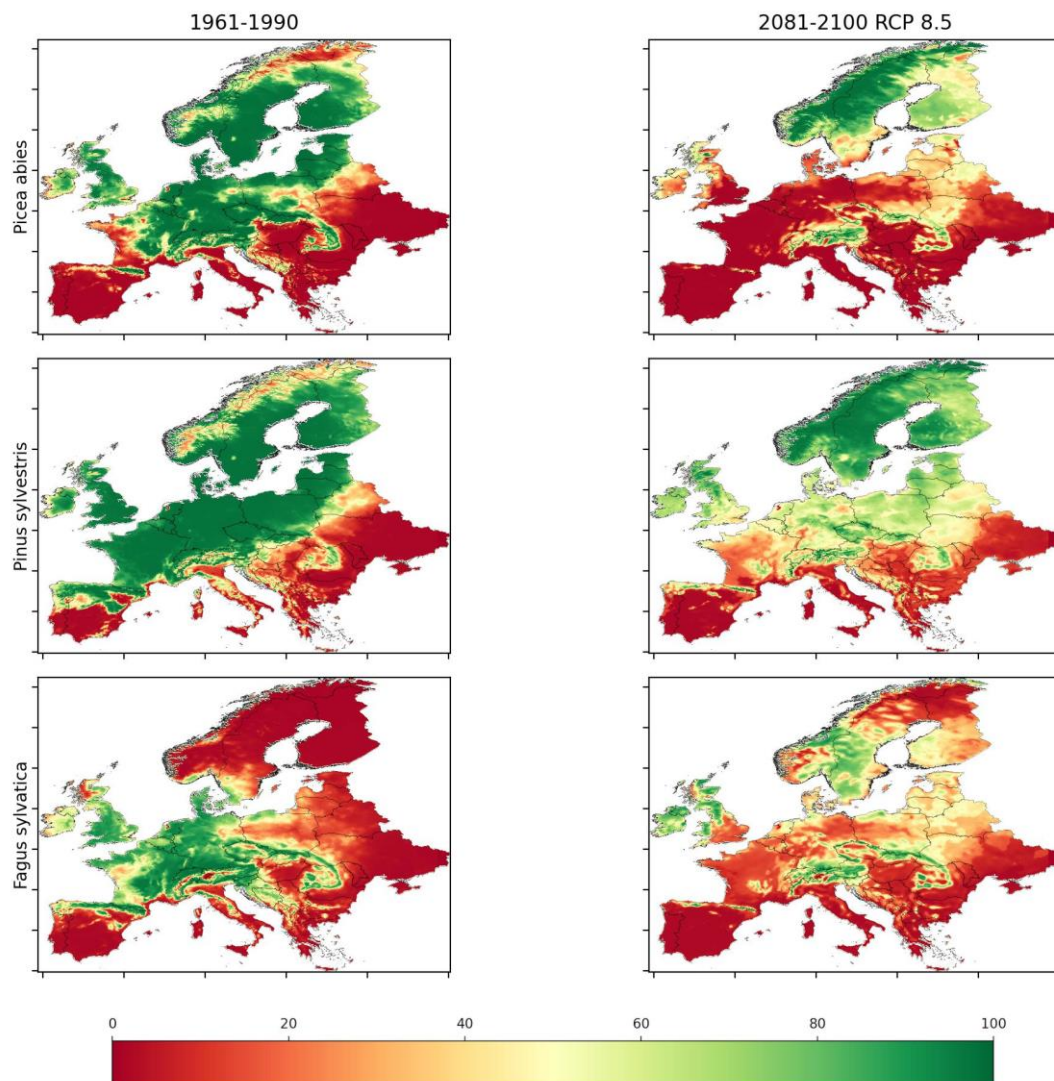


**Figure 2: Probability of tree species distribution [0 to 100%] under the historical period (1961-1990) and predicted future scenario of 2080-2100 under RCP 8.5.**

### 3.4 Climate and weather risks

Two main methodological approaches are pursued in this project:

- (1) analysis of the interdependencies between forest disturbances and exposure to climatic conditions;
- (2) computation of bioclimatic similarities between well-known Austrian regions and forest areas across Europe.

#### 3.4.1 Forest damage

Data on forest disturbances is essential for modelling forest damages. In Austria, the Austrian Research Center for Forests (BFW) collects data on damage volumes and areas on an annual basis for every forest district. Information of over 60 biotic and abiotic damage types is collected in this database. Given the



expected climatic changes, the focus of this project is on damages caused by drought and the bark beetle as well as wind and snow.

In order to link climatological conditions with actual impacts in terms of forest disturbances, data on forest damages need to be collected. The main source of information is the documentation of forest damages in Austria, as compiled by the BFW. It includes data on forest disturbances, which are collected annually since 2002 on a district level. In addition, the European Database on Forest Disturbances (DFDE) has been analysed. Data contained in this database are derived from literature reviews and are solely available as aggregations over countries on temporal resolutions between years and decades. Due to both the rough as well as inconsistent spatial and temporal resolution, these data do not provide the anticipated added value and are hence not used for further analyses.

In order to consider the species affected by the respective damage types, BFW damage data was linked with data on species distribution as collected during the latest forest inventory in Austria. As a starting point, only spruce damage was considered. By using the damage class (volume or area, depending on the damage type) as a target variable and various independent input features, random forest models were trained in order to predict the relative damage for each of the selected damage types.

The following independent variables were considered:

- 11 bioclimatic indicators on temperature
- 8 bioclimatic indicators on precipitation
- Available breeding material
- lagged damage (total damages of the previous year)
- information on elevation (minimum, maximum and range)
- information on growing areas

The model setup comprises a nested resampling procedure, using a proper train-validation-test split. Hyperparameter tuning was performed by employing model-based Bayesian optimization, using Kriging as a surrogate learner.

Due to the comprehensive data basis, models can be set up separately for all nine of Austria's main forest growing areas ("*Forstliche Wuchsgebiete*").

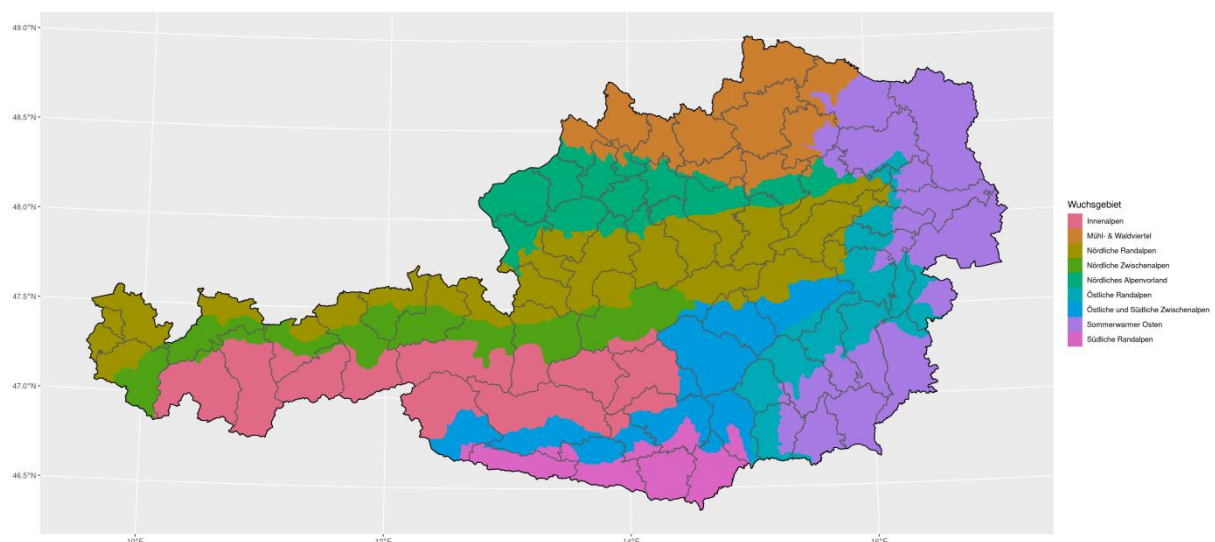


**Figure 3: Overview over major forest growing areas and forest districts.**

### 3.4.2 Identification of similar climatological regions based on 19 bioclimatic variables

#### Data

Bioclimatic variables are derived from monthly temperature and precipitation values to yield biologically meaningful variables. These are commonly used in species distribution modeling and ecological modeling techniques. The bioclimatic variables represent annual trends (e.g. mean annual temperature, annual precipitation), seasonality (e.g. annual variation in temperature and precipitation), and extreme or limiting environmental factors (e.g. temperature of the coldest and warmest month and precipitation of the wettest and driest quarter). A quarter covers a period of three months. The 19 bioclimatic variables used in the course of the project are listed in Table 2.

**Table 2: Definitions of considered bioclimatic variables**

Abbreviation	Definiton
BIO1	Annual mean temperature
BIO2	Mean Diurnal Range (Mean of monthly (max temp – min temp))
BIO3	Isothermality (BIO2/BIO7)*100
BIO4	Temperature Seasonality (standard deviation * 100)
BIO5	Max Temperature of Warmest Month
BIO6	Min Temperature of Coldest Month
BIO7	Temperature Annual Range (BIO5-BIO6)
BIO8	Mean Temperature of Wettest Quarter
BIO9	Mean Temperature of Driest Quarter
BIO10	Mean Temperature of Warmest Quarter
BIO11	Mean Temperature of Coldest Quarter
BIO12	Annual Precipitation
BIO13	Precipitation of Wettest Month
BIO14	Precipitation of Driest Month
BIO15	Precipitation Seasonality (Coefficient of Variation)
BIO16	Precipitation of Wettest Quarter
BIO17	Precipitation of Driest Quarter
BIO18	Precipitation of Warmest Quarter
BIO19	Precipitation of Coldest Quarter

**Table 3: Global Circulation Models (GCMs) considered in this study**

GCM	SSP1-26	SSP2-45	SSP3-70	SSP5-85
BCC-CSM2-MR	X	x	X	X
CNRM-CM6-1	X	X	X	X
CNRM-ESM2-1	X	X	X	X
CanESM5	X	X	X	X
GFDL-ESM4	X		X	
IPSL-CM6A-LR	X	X	X	X
MIROC-ES2L	X	X	X	X
MIROC6	X	X	X	X
MRI-ESM2-0	x	X	x	X

#### Past

For the past climate conditions in the growing areas considered in this study, the 19 bioclimatic variables in the Worldclim database are available at 2.5 arcmin resolution as means over the period 1971-2000 (Fick and Hijmans, 2017).

### Future

The mean values of the considered bioclimatic parameters are globally available for the scenarios SSP1-26, SSP2-45, SSP3-70 and SSP5-85, and for the periods 2021--2040, 2041--2060, 2061--2080 and 2081--2100. The spatial resolution is 2.5 arcminutes. An overview of the global circulation models (GCMs) considered and their availability are given in Table 3.

### Calculation

For the target region under consideration (single growing areas) the bioclimatic parameters were determined for the 30-year period 1970-2000 and the spatial mean of all 19 considered bioclimatic variables was calculated. The resulting 19-dimensional vector was now used to identify regions in Europe where similar climatic conditions are to be expected in the future as they were predominant in the Mühl- and Waldviertel in the past.

The Euclidean distance is used as a similarity measure. For the calculation of this, the European-wide earth surface is divided into windows with a size of 20 times 20 (size of the growth area Mühl- und Waldviertel) grid points, and a spatial moving average is determined. Thus, at each grid point there is a 19-dimensional vector representing the mean conditions in each box. In addition, before the Euclidean distance is determined, all vectors considered (vector in the growth area in the past and Europe-wide in the future) are scaled with the past values (spatial mean and standard deviation). After this standardization, the Euclidean distance is calculated and stored for each grid point.

Calculations have been conducted for the scenarios SSP1-26, SSP2-45, SSP3-70 and SSP5-85 and the 20-year periods 2021–2040, 2041–2060, 2061–2080 and 2081–2100.

The Euclidean distance  $d(p, q)$  between two points  $p$  and  $q$  is defined as the Euclidean norm  $\|q - p\|_2$  of the difference vector between the two points. For the two points  $p$  and  $q$  with the coordinates  $p = p_1, p_2, \dots, p_n$  and  $q = q_1, q_2, \dots, q_n$  applies (in the case of 19 bioclimatic indicators with  $n = 19$ ):

$$d(p, q) = \|q - p\|_2 = \sqrt{(q_1 - p_1)^2 + \dots + (q_n - p_n)^2} = \sqrt{\sum_{i=1}^n (q_i - p_i)^2}$$

### 3.4.3 Identification of similar climatological regions based on the ECLIPS2.0 dataset

#### Data

The ECLIPS2.0 dataset (Chakraborty et al., 2020) is a high-resolution gridded dataset that includes a variety of bioclimatic variables and is based on the EURO-CORDEX dataset. Gridded data comprises 80 annual, seasonal, and monthly climatic variables for two past (1961-1990, 1991-2010) and five future (2011-2020, 2021-2040, 2041-2060, 2061-2080, and 2081-2100) time periods. The future data are based on five different RCMs driven by two climate scenarios - RCP4.5 and RCP8.5. Two ECLIPS versions have been developed: ECLIPS 1.1 with a spatial resolution of  $0.11^\circ \times 0.11^\circ$ , which is the resolution of the underlying RCMs, and ECLIPS 2.0, which was downscaled to a resolution of 30 arcseconds using the delta approach. For the calculation within the 'Forest Risk Map' project, the ECLIPS 2.0 version was used. It is available as single TIFs of included parameters for the respective scenarios and time periods and can be downloaded from <https://doi.org/10.5281/zenodo.3952159>. Table 4 gives an overview of included indices and respective definitions.

**Table 4: Climate indices calculated based on the ECLIPS1.1 and 2.0 dataset using the bias-corrected daily time series of the EURO-CORDEX data.**

Acronym	Variable name	Unit	Calculation
MWMT	Mean warmest month temperature	°C	$MWMT = \max(T_{mon.mean})$
MCMT	Mean coldest month temperature	°C	$MCMT = \min(T_{mon.mean})$
TD	Continentalinity	°C	$MWMT - MCMT$

<i>AHM</i>	Annual index	heat:moisture	°C/mm	$AHM = \frac{MAT + 10}{MAP/1000}$
<i>SHM</i>	Summer index	heat:moisture	°C/mm	$SHM = \frac{MWM T}{MSP/1000}$
<i>DDbelow0</i>	Degree-days below 0°C		°C	$DDbelow0 = \sum_{doy} \begin{cases} T, & T < 0^{\circ}C \\ 0^{\circ}C, & T > 0^{\circ}C \end{cases}$
<i>DDabove5</i>	Degree-days above 5°C		°C	$DDabove5 = \sum_{doy} \begin{cases} T - 5^{\circ}C, & T > 5^{\circ}C \\ 0^{\circ}C, & T < 5^{\circ}C \end{cases}$
<i>DDbelow18</i>	Degree-days below 18°C		°C	$DDb18 = \sum_{doy} \begin{cases} T - 18^{\circ}C, & T < 18^{\circ}C \\ 0^{\circ}C, & T > 18^{\circ}C \end{cases}$
<i>DDabove18</i>	Degree-days above 18°C		°C	$DDbelow18 = \sum_{doy} \begin{cases} T - 18^{\circ}C, & T > 18^{\circ}C \\ 0^{\circ}C, & T < 18^{\circ}C \end{cases}$
<i>NFFD</i>	Number of days	frost-free	-	$NFFD = \sum_{doy} \begin{cases} 1, & T_{min} > 0^{\circ}C \\ 0, & T_{min} < 0^{\circ}C \end{cases}$
<i>FFP</i>	Longest frost-free period		days	The length of the longest period in the year when the daily minimum temperature is above 0°C for consecutive days.
<i>bFFP</i>	Beginning of FFP		day	First calendar day when the longest frost-free period starts.
<i>eFFP</i>	End of FFP		day	The last calendar day when the longest frost-free period ends.
<i>EMT</i>	Extreme temperature	minimum	°C	$EMT = \min(T_{min})$
<i>MAT</i>	Annual temperature	mean	°C	Average of daily mean temperature over a year
<i>MAP</i>	Annual precipitation	total	mm	Summary of daily precipitation over a year
<i>Tmin_an</i>	Annual minimum temperature	mean of	°C	Average of daily minimum temperature over a year
<i>Tmax_an</i>	Annual maximum temperature	mean of	°C	Average of daily maximum temperature over a year
<i>Tmax_01 to Tmax_12</i>	Maximum temperatures	monthly	°C	Average of daily maximum temperature over a month
<i>Tmin_01 to Tmin_12</i>	Minimum temperatures	monthly	°C	Average of daily maximum temperature over a month
<i>Tave_01 to Tave_12</i>	Mean temperatures	monthly	°C	Average of daily mean temperature over a month
<i>Tave_at</i>	Mean temperature	autumn	°C	Average of daily mean temperature for Sep-Nov
<i>Tave_sm</i>	Mean temperature	summer	°C	Average of daily mean temperature for Jun-Aug
<i>Tave_sp</i>	Mean temperature	spring	°C	Average of daily mean temperature for Mar-May
<i>Tave_wt</i>	Mean temperature	winter	°C	Average of daily mean temperature for Dec of previous year to Feb
<i>Tmax_at</i>	Maximum temperature	autumn	°C	Average of daily maximum temperature for Sep-Nov
<i>Tmax_sm</i>	Maximum temperature	summer	°C	Average of daily maximum temperature for Jun-Aug
<i>Tmax_sp</i>	Maximum temperature	spring	°C	Average of daily maximum temperature for Mar-May
<i>Tmax_wt</i>	Maximum temperature	winter	°C	Average of daily maximum temperature for Dec of previous year to Feb
<i>Tmin_at</i>	Minimum temperature	autumn	°C	Average of daily maximum temperature for Sep-Nov
<i>Tmin_sm</i>	Minimum temperature	summer	°C	Average of daily maximum temperature for Jun-Aug
<i>Tmin_sp</i>	Minimum temperature	spring	°C	Average of daily maximum temperature for Mar-May
<i>Tmin_wt</i>	Minimum temperature	winter	°C	Average of daily maximum temperature for Dec of previous year to Feb
<i>PPT_at</i>	Mean precipitation	autumn	mm	Average of daily mean precipitation for Sep-Nov
<i>PPT_sm</i>	Mean precipitation	summer	mm	Average of daily mean precipitation for Jun-Aug
<i>PPT_sp</i>	Mean precipitation	spring	mm	Average of daily mean precipitation for March-May
<i>PPT_wt</i>	Mean precipitation	winter	mm	Average of daily mean precipitation for Dec of previous year to Feb
<i>PPT_01 to PPT_12</i>	Mean precipitation	monthly	mm	Average of the daily precipitation sums for a month



The climate indices listed in Table 1 are available for the following RCMS:

- CLMcom CCLM
- CLMcom CLM
- DMI HIRHAM
- KMNI RACMO
- MPI CSC REMO2009

#### Calculation

The overall methodology applied is very similar to the method used for the bioclimatic variables. The main difference is the dimensionality reduction applied as an additional processing step at the beginning of the analysis.

Due to the high number of parameters represented in the ECLIPS dataset, a Principal Component Analysis (PCA) was performed as a first step, prior to the calculation of climatically similar regions. This dimension reduction allows the identification of regions based on only the first two Principal Components (PCs); these together exhibit an explained variance of more than 80% (see Scree Plot, Fig. 4). PC1 and PC2 are vectors with 80 components each; these represent the climate indices included in the dataset. The values of the entries show the importance of the individual indices, as illustrated in Figure 5.

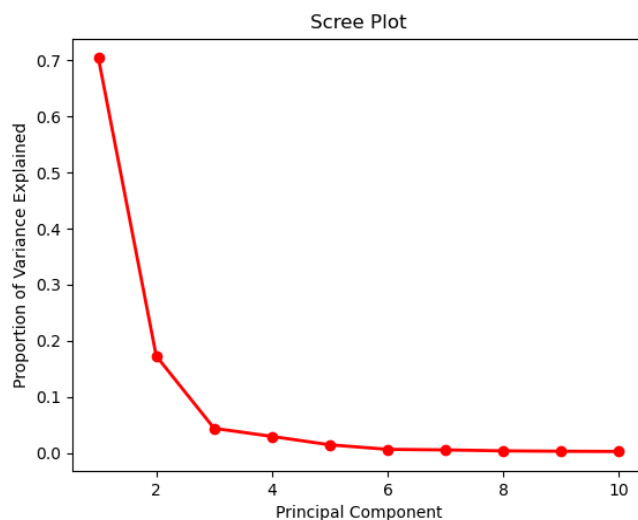


**Figure 4: Scree plot of PCA based on ECLIPS2.0 data over the period 1991 - 2010. The first two Principal Components together represent over 80% of the variability of all 82 climate indices.**

For the target region under consideration (growing area Mühl- and Waldviertel), the spatial mean of all 80 considered bioclimatic variables was computed. PC1 and PC2 were determined for the 20-year period 1991-2010. The resulting vector was now used to identify regions in Europe where similar climatic conditions are to be expected in the future as they were predominant in the Mühl- and Waldviertel in the past.

The Euclidean distance is used as a similarity measure. For the calculation of this, the European-wide earth surface is divided into windows with the size of the growth area Mühl- und Waldviertel), a spatial moving average is determined and the PCA conducted for the past conditions was applied to each box over Europe. Thus, at each grid point there is a 160-dimensional vector (2 times 80 – PC1 and PC2 in one vector) representing the mean conditions in each box. Thereafter, the Euclidean distance is calculated and stored for each grid point.

Calculations have been conducted for the scenarios RCP4.5 and RCP8.5 and the 20-year periods 2021-2040, 2041-2060, 2061-2080 and 2081-2100.

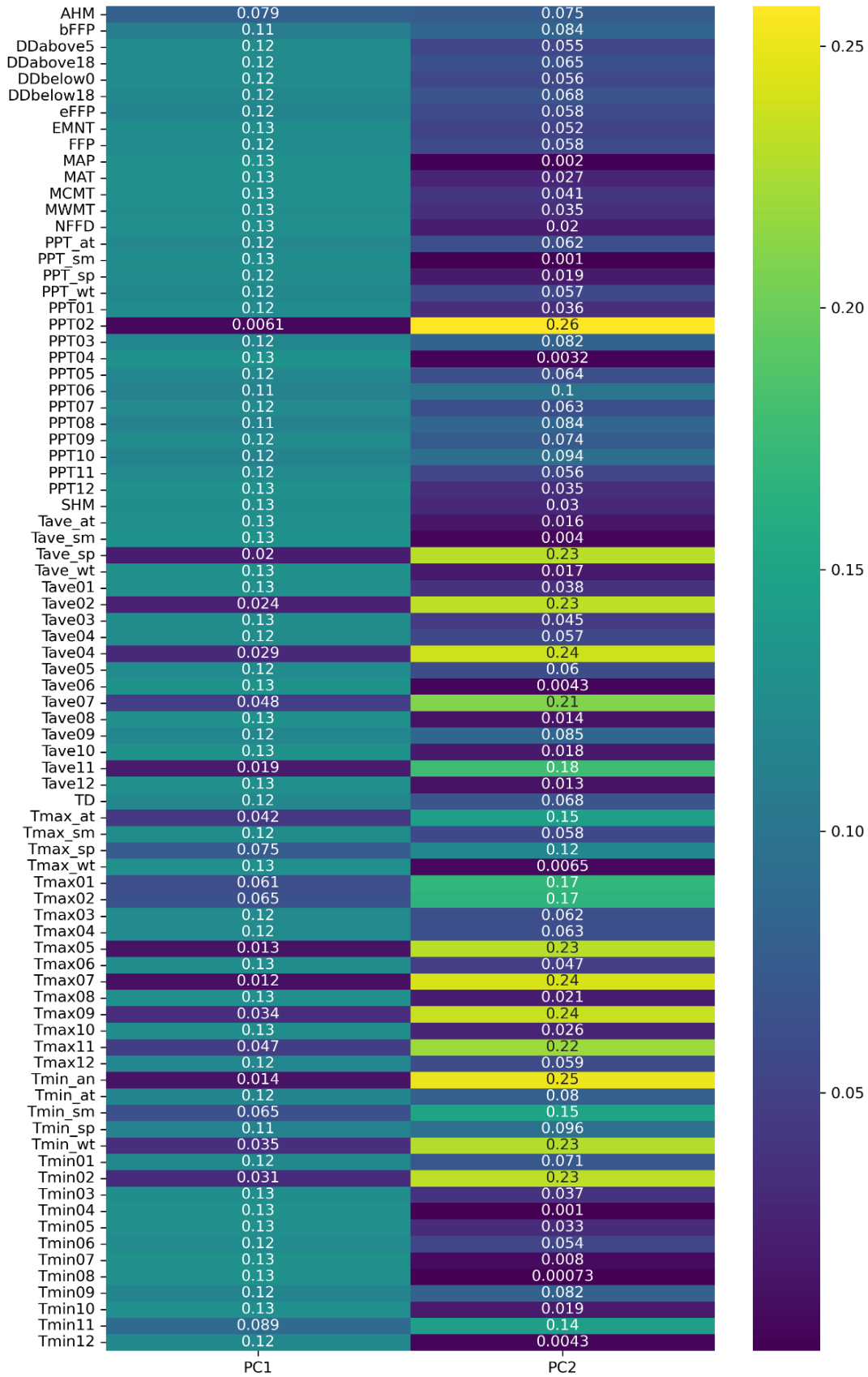


Figure 5.: Contribution of the individual climate indices to PC1 and PC2.

### 3.5 Risk Map Calculation

The input parameter for the calculation and representation of future potential stocks, the stock change, and the risk-values were the following:

1. Current stocks available on NUTS2 Level (see 3.2) for single tree species
2. The probability of species occurrence as modelled with species distribution models (3.3) available as raster data for each species (Norway spruce, Scots pine, and European beech) for present and future climate (Fig. 2.)
3. Current species shares available as raster data.

The first step was the reduction of the future probability of species occurrence to the actual species share (Fig. 6) within the respective area (pixel). In the second step, the pixel data were aggregated for each NUTS2 region by calculating the median of all pixel values within the respective NUTS2 region (Fig. 7).

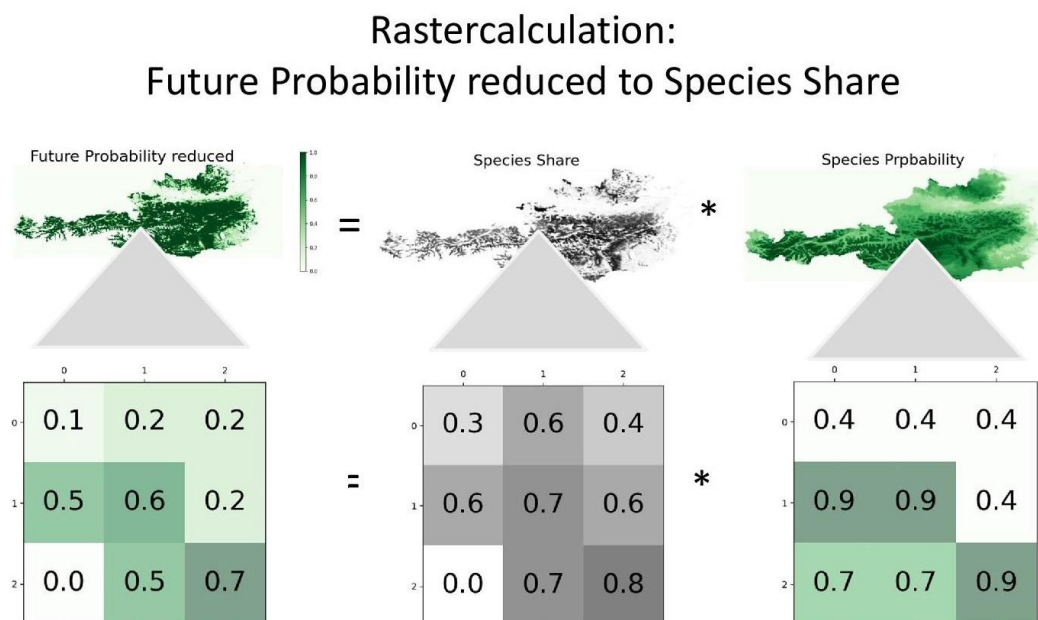


**Figure 6: Calculation of future probability of occurrence reduced to species share for each pixel.**

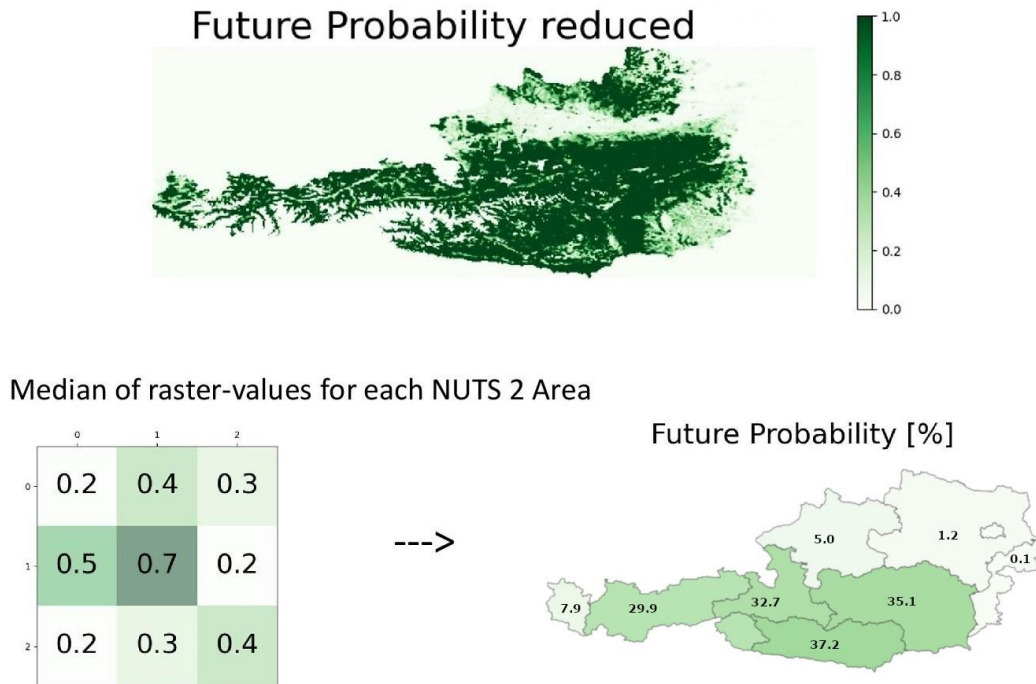


**Figure 7: Calculation of the future probability of occurrence for each NUTS2 region.**

To estimate the potential future stock, we assumed the same ratio of current stock to current probability of occurrence as for future stock to future probability of occurrence. Following this approach, we calculated the potential stocks following this formula (Fig. 8).

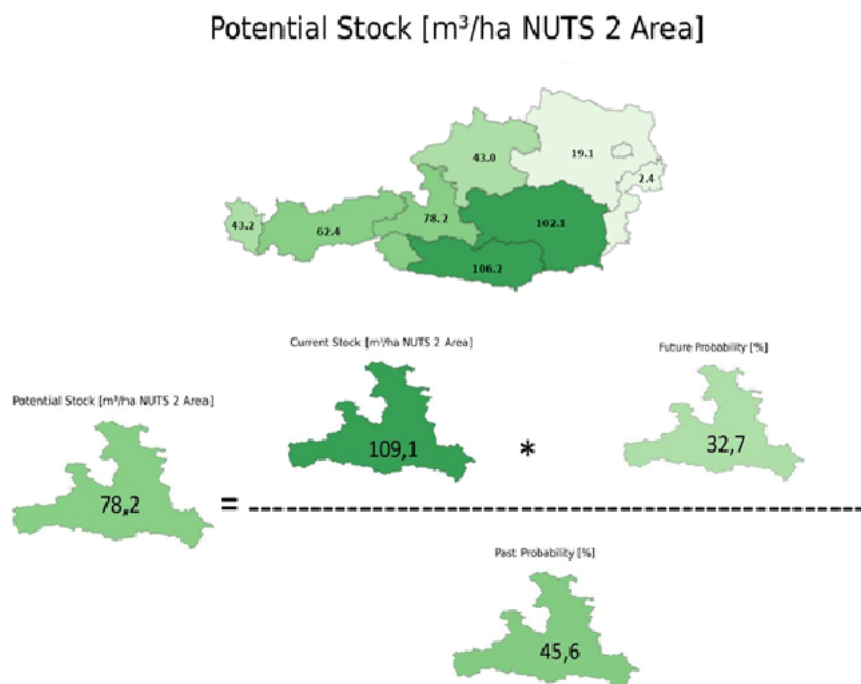


**Figure 8: Calculation of the potential future stock in 2081 under the RCP8.5 climate scenario for each NUTS2 area. The calculation of the absolute values [mill. m<sup>3</sup>] follows the same approach.**

On basis of the estimated current stock and the potential future stock, we calculated the stock change in million m<sup>3</sup> for each total NUTS2 region and in m<sup>3</sup>/ha as average of each region (Fig. 9). Furthermore, the ratio of the stock change in relation to the current stock was quantified in percent change (Fig. 10).

### Stock Change [m<sup>3</sup>/ha NUTS 2 area]

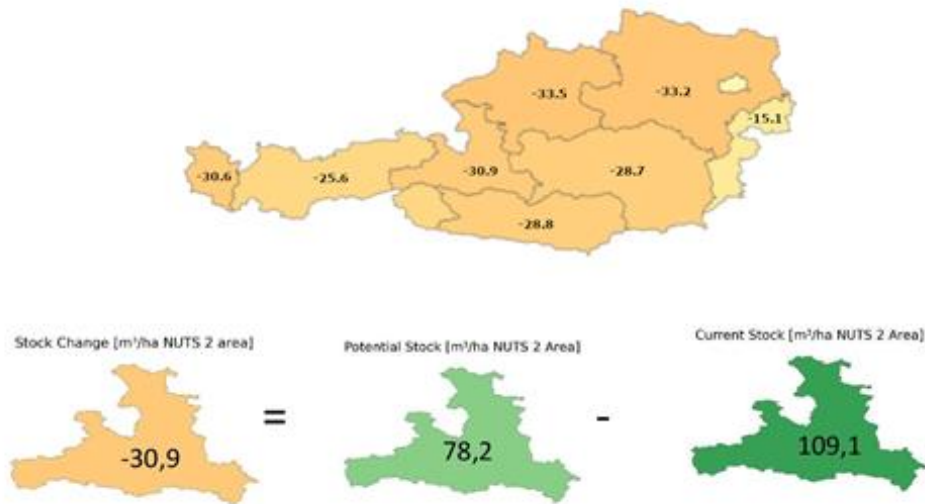


Figure 9: Calculation of the stock change in 2081 under the RCP8.5 climate scenario for each NUTS2 area. The calculation of the absolute values [mill. m<sup>3</sup>] follows the same approach.

### Stock Change [% of Current Stock]

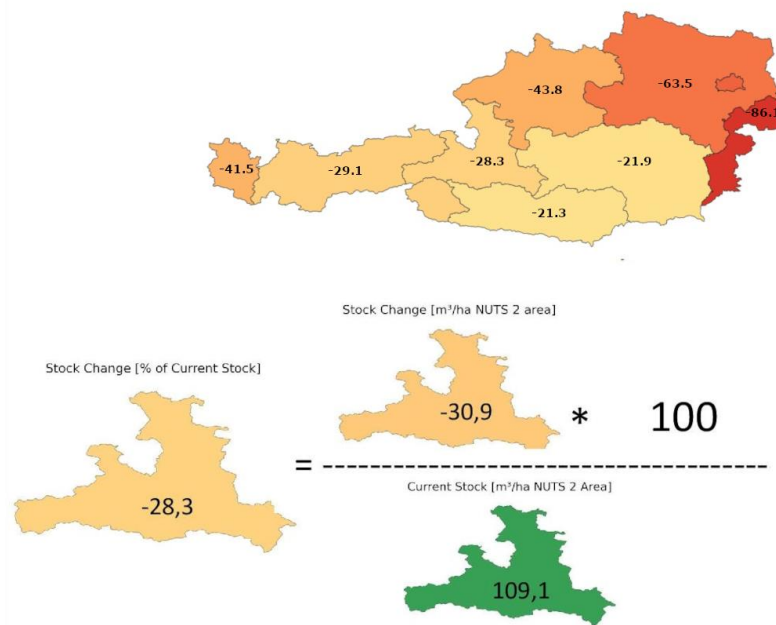


Figure 10: Calculation of the stock change as the rate of the current stock in 2081 under the RCP8.5 climate scenario for each NUTS2 area.

To estimate the overall risk for each species, we transferred the probability of occurrence of a given species under a given climate change scenario into its reverse values, the probability of failure [%] by taking the respective actual species share within a given area into account (Fig. 11). To accumulate the data of each pixel to represent a given NUTS2 region, we choose the median of all the pixels within that region (Fig. 12).

To calculate the future risk, i.e. the probability of failure for all species we multiplied the values of each species.

We not only expressed the risk through a probability, but calculated values considering the current stock, by taking the probability times the stock.

### Rastercalculation: Future Risk

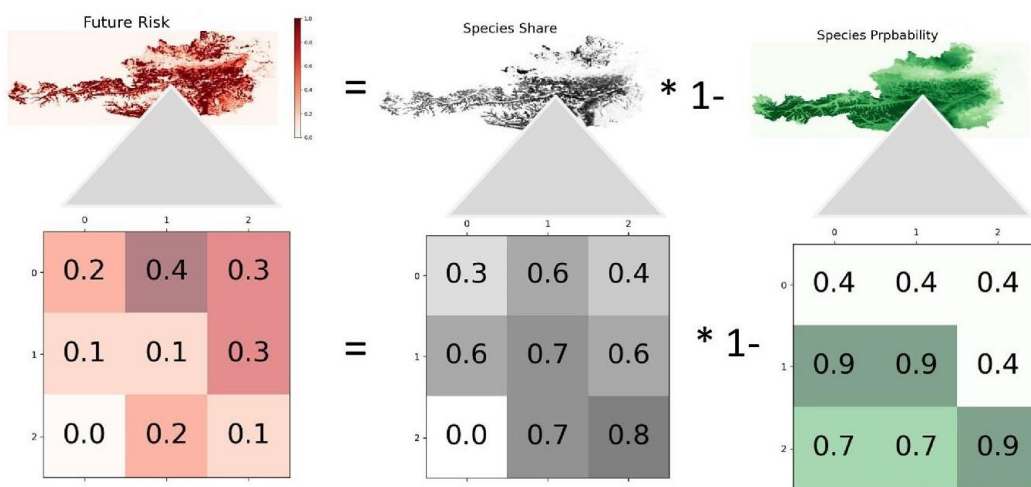


Figure 11: Calculation of future risk for each pixel.

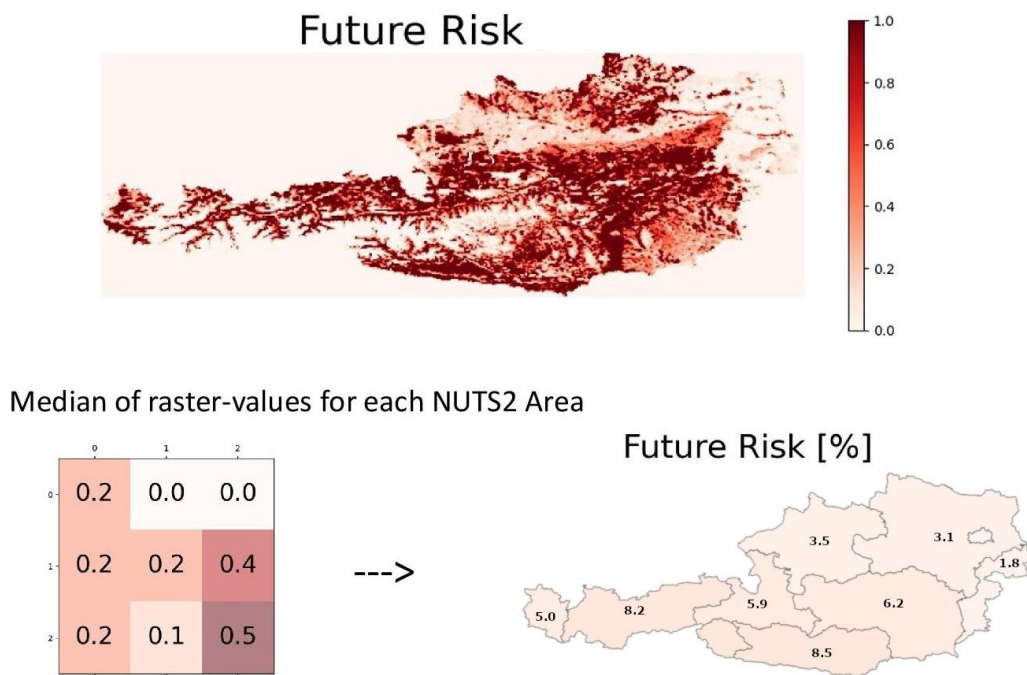


Figure 12: Calculation of future risk for each NUTS2 region.



Table 5: Summary of calculation formulae.

Values		Calculation
Current Stock of one Species	[mill. m <sup>3</sup> ]	current stock [m <sup>3</sup> ]/1000000
Current Stock of of all species	[mill. m <sup>3</sup> ]	added species current stocks
Potential Stock in the future of one Species	[mill. m <sup>3</sup> ]	current stock [mill.m <sup>3</sup> ]*((future species probability/100)/(past species probability/100)
Potential Stock in the future of all species	[mill. m <sup>3</sup> ]	added species Potential Stocks
Stock Change one Species	[mill. m <sup>3</sup> ]	current stock [mill.m <sup>3</sup> ]- potential stock [mill.m <sup>3</sup> ]
Stock Change all species	[mill. m <sup>3</sup> ]	added species Stock Changes
Ratio of Stock Change one Species	[%]	stock change species [mill.m <sup>3</sup> ]*100/actual stock species [mill.m <sup>3</sup> ]
Ratio of Stock Change all species	[%]	stock change total [mill.m <sup>3</sup> ]*100/actual stock all species [mill.m <sup>3</sup> ]
Current Stock of one Species	[m <sup>3</sup> /ha]	current stock [m <sup>3</sup> /ha]
Current Stock of of all species	[m <sup>3</sup> /ha]	added species current stocks
Potential Stock one Species	[m <sup>3</sup> /ha]	actual stock/ha*((future species probability/1000)/(past species probability/1000)
Potential Stock all species	[m <sup>3</sup> /ha]	added species Potential Stocks
Stock Change one Species	[m <sup>3</sup> /ha]	current stock- potential stock
Stock Change all species	[m <sup>3</sup> /ha]	added species stock changes
Riskvalue one species	[m <sup>3</sup> /ha]	("species share" / 100 ) * ( 100 – "Future species probability") * current stock [m <sup>3</sup> /ha]
Riskvalue all species	[m <sup>3</sup> /ha]	added Riskvalues of all species
Riskvalue one species	[mill. m <sup>3</sup> ]	("species share" / 100 ) * ( 100 – "Future species probability") * current stock [mill. m <sup>3</sup> ]
Riskvalue all species	[mill. m <sup>3</sup> ]	added Riskvalues of all species
Riskvalue Share one species	[%]	("species share" / 100 ) * ( 100 – "Future species probability")
Riskvalue Share all species	[%]	multiplied Riskvalues [%] of all species

## 4 Results

### 4.1 Current forest stocks

#### 4.1.1 Growing stock in Austria

The growing stock results obtained from the Austrian NFI data are presented in terms of volume in Figure 13 and as above-ground biomass (AGB) in Figure 14, both per ha of BFI area. The results show a clear dominance of coniferous growing stock. Norway spruce contributes the largest part to the growing stock. Among broadleaves, beech has a comparably large share.

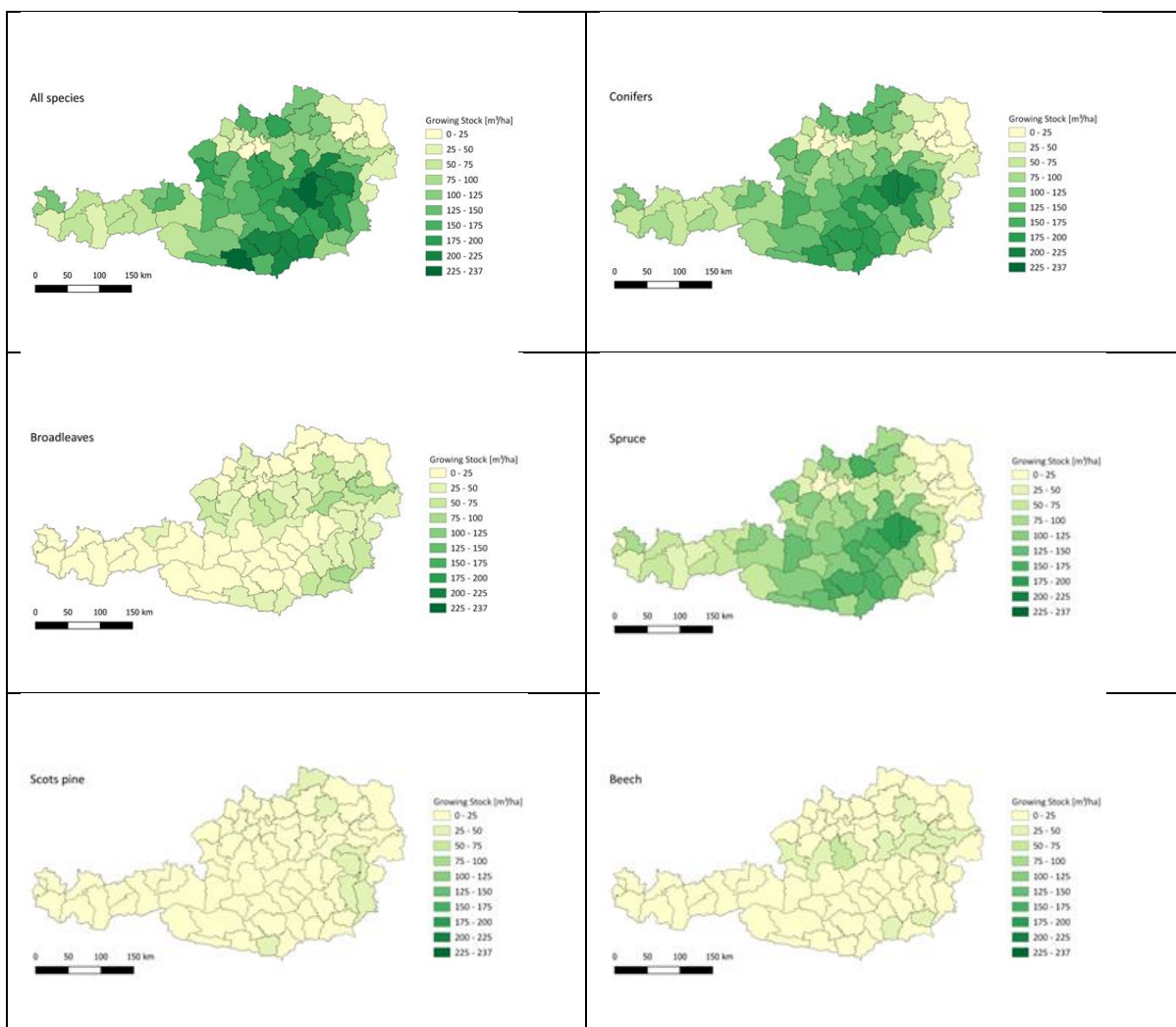


Figure 13: Growing stock volume in m³/ha by tree species for BFIs in Austria.



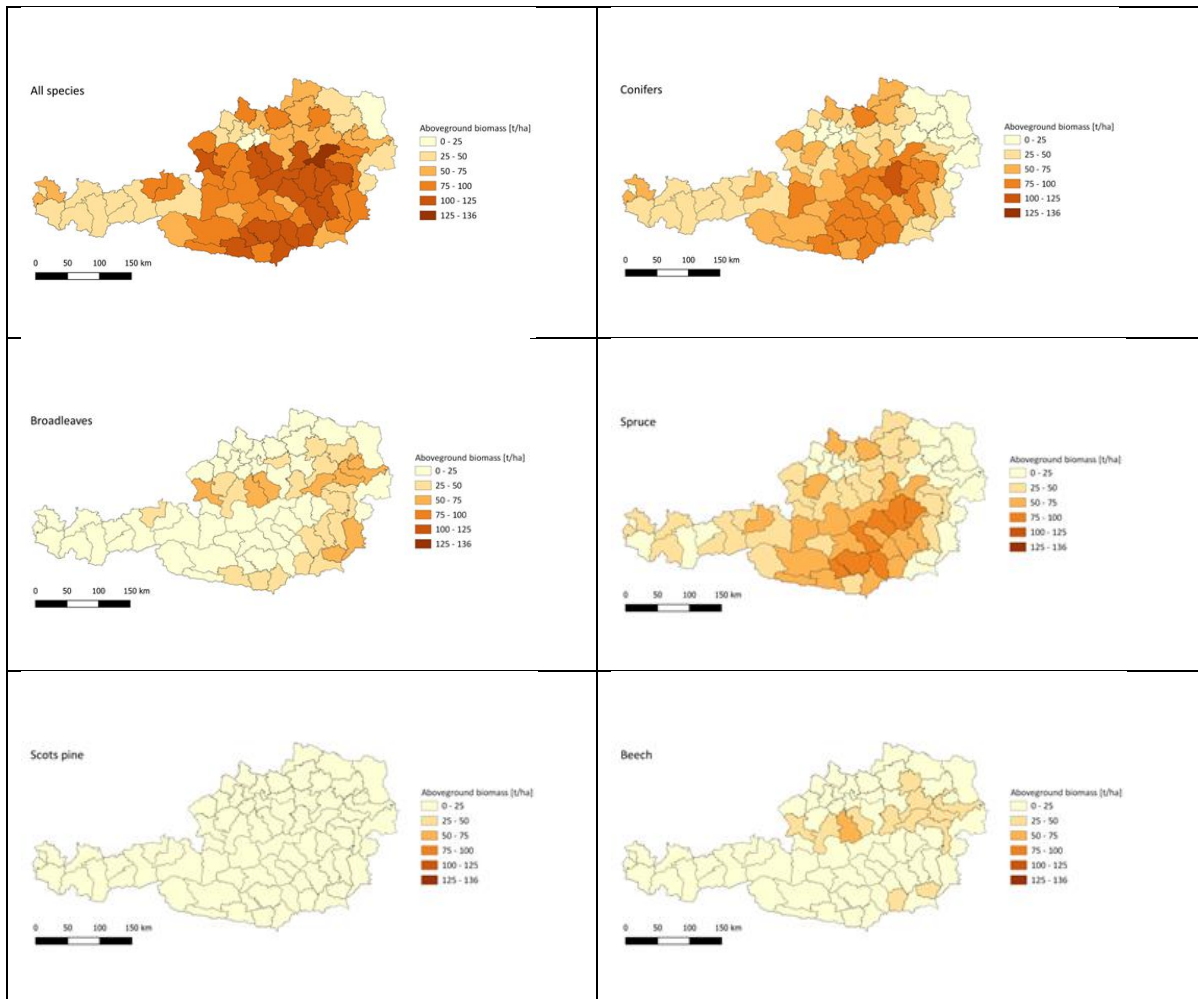


Figure 14: Growing stock AGB in t/ha by tree species for BFIs in Austria.

#### 4.1.2 Growing stock in Europe

Figures 15 and 16 display the growing stock distribution derived from the FRA 2020 data and the data of Santoro (2018) and Bruce et al. (2011). For the purpose of mapping, the growing stocks are presented in  $\text{m}^3/\text{ha}$  and  $\text{t}/\text{ha}$  per area of NUTS2 regions. The NUTS classification is not available for Belarus and Ukraine, thus hampering a differentiation of smaller area entities such as NUTS2. A new subdivision of these countries comparable to the NUTS classification would exceed the scope of this project and thus these countries are treated as a single unit. However, the identical methodology is applied and the only difference to the NUTS2 regions is the coarser spatial resolution. Estonia and Latvia are also not divided, because they only have subdivisions on NUTS3-level, but not on NUTS2.

Total growing stocks in  $\text{m}^3$  and  $\text{t}$  are available for further processing and risk assessment as described in the following sections. The results show high growing stocks in Central Europe and also in the Carpathian region. Coniferous growing stock is dominant in Central and Northern Europe, whereas broadleaved tree species are more prevalent in Southeastern Europe and Western Europe. Norway spruce has the highest growing stocks in Central Europe and partly also in Northern Europe. The growing stocks of Scots pine are mainly occurring in the Northeastern part of Europe.

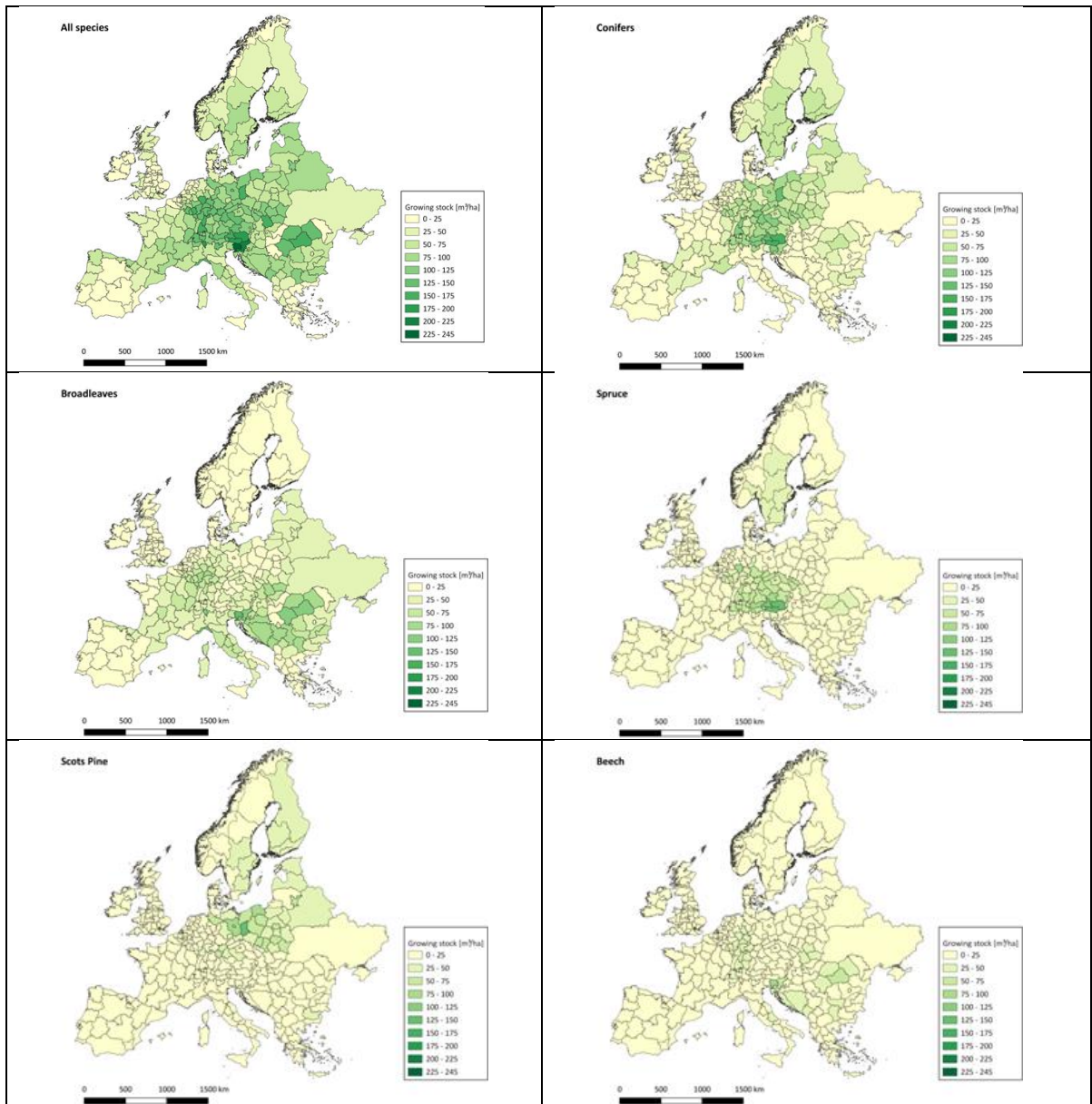


Figure 15: Growing stock volume in m³/ha by tree species for NUTS2 regions in Europe.

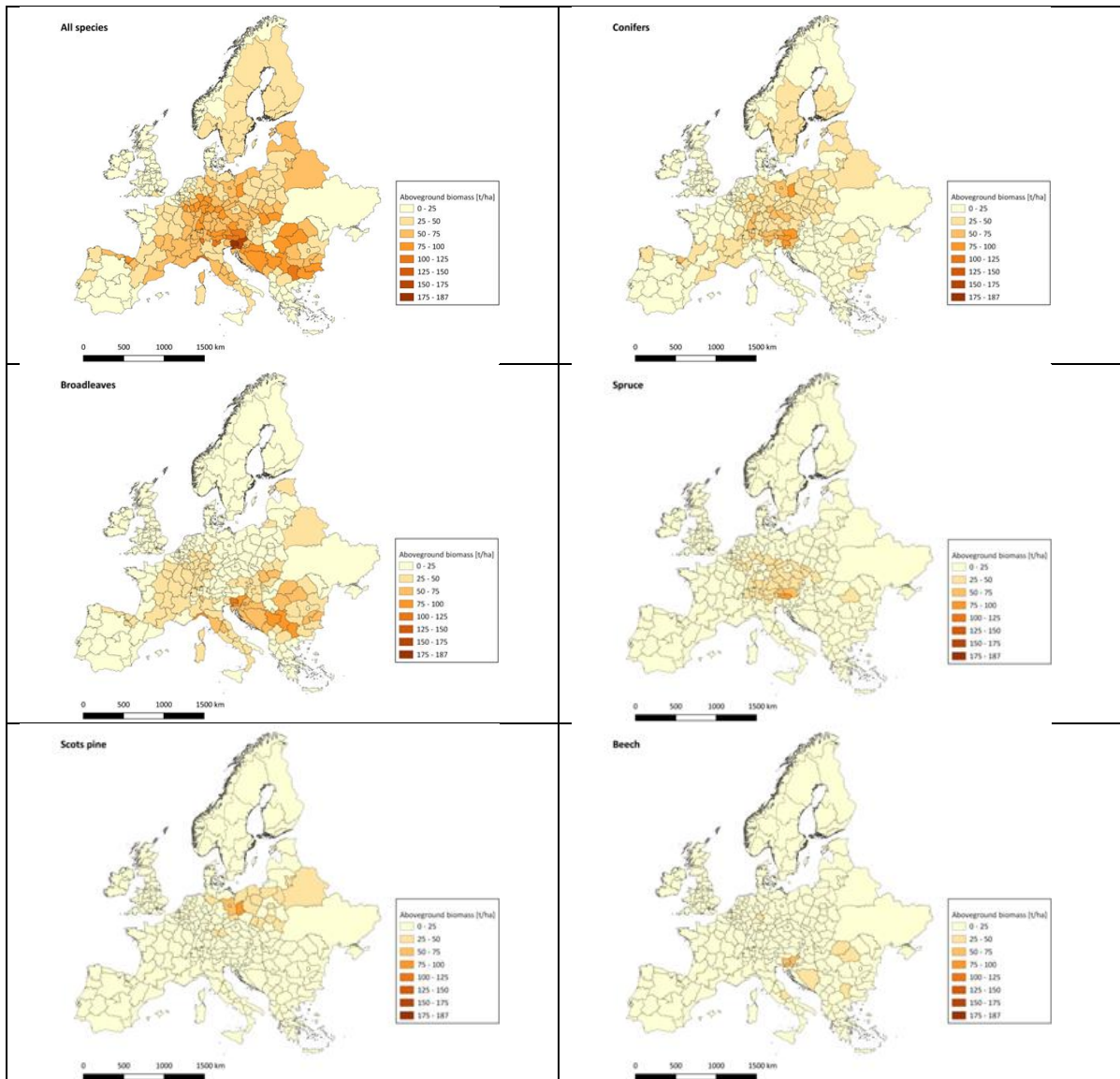


Figure 16: AGB in t/ha by tree species for NUTS2 regions in Europe.

#### 4.1.3 Uncertainty

The comparison of growing stock results derived from the Santoro (2018) and Bruce et al. (2011) datasets with the results from the Austrian NFI revealed an overestimation by the former. The over-estimation is due to two main reasons:

- 1) Estimates are higher because of the full coverage of the remote sensing data, whereas the terrestrial Austrian NFI does not survey some areas that are inaccessible and therefore no data is available. Also, some stocked areas outside forests are not classified as forest and thus ignored.
- 2) In high elevation areas there is shrub forest with low growing stocks but it is likely interpreted as regular forest in satellite images.

When correcting for the inaccessible forest area for the Austrian data, the main part of the differences is accounted for (Figure 17).

The validation shows that the Santoro dataset is a reliable source with some uncertainty. A 20% confidence interval on NUTS2-level can be assumed for the stock estimates. A similar effect like at the altitudinal timberline in Austria was also found for the latitudinal timberline in Northern Europe, where the results from Santoro (2018) and Bruce et al. (2011) datasets showed overestimation compared to the FRA 2020 results. However, through the chosen approach of using FRA 2020 data as basis and deriving the

growing stock distribution over NUTS2 regions, from Santoro (2018) and Bruce et al. (2011), a reduction of such effects is expected.

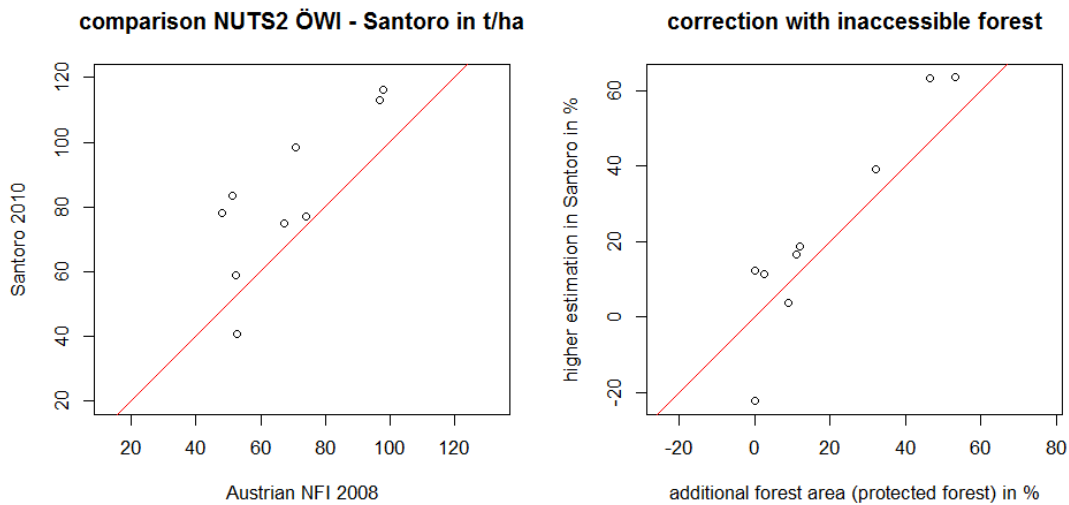


**Figure 17: Comparing Santoro (2018) and Austrian NFI results for NUTS2 regions, first directly and then with correction because of inaccessible forest.**

## 4.2 Climate and weather risks

### 4.2.1 Damage models

Results indicate varying performance, which strongly depends on the damage category under consideration. This is attributed to two effects. First, the number of events recorded in the database is varies greatly between the different categories. Some damage types are documented well, other exhibit only very few damage events, or extremely low amounts of damage (when considering the relative damage in the total forest district). Second, the used bioclimatic variables are not equally well suited for all damage types. Especially damage categories, which are related to weather effects that are insufficiently captured by the 19 bioclimatic variables (e.g. hail, storm) are difficult to model. Consequently, adjustments to the types of input variables used are currently under consideration.

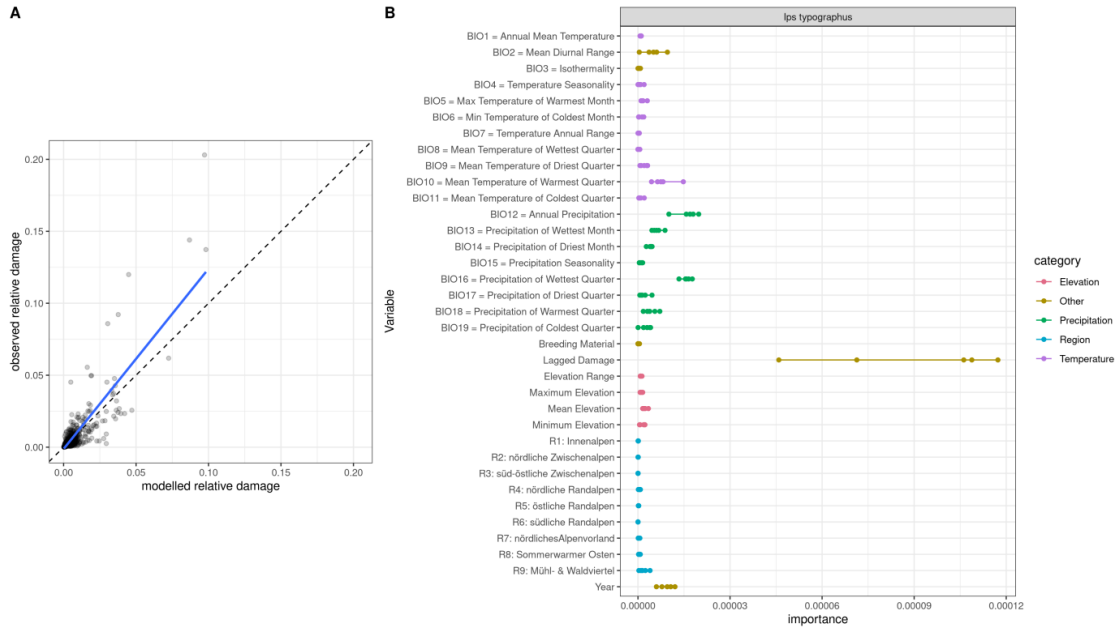


**Figure 18: Random forest model for *Ips typographus*.** Panel (A) shows the predicted versus observed relative damage ( $R^2 = 0.721$ ), indicating a good performance, but also a slight underestimation of large damages. Panel (B) exhibits the feature importance of the independent variables, with lagged damage showing the biggest feature importance.

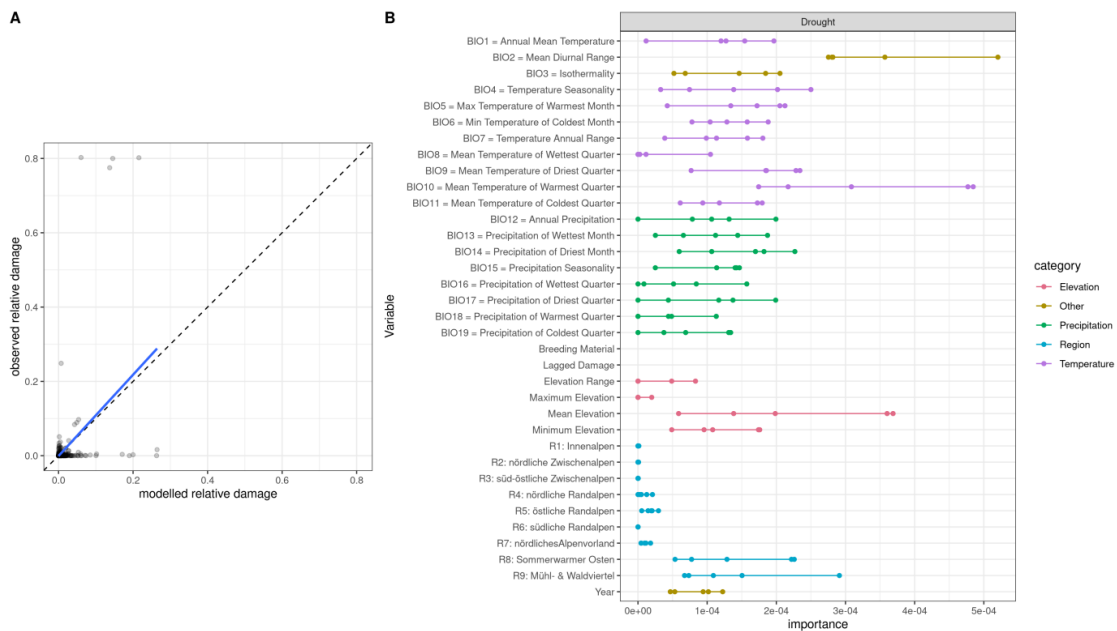


**Figure 19: Random forest model for droughts.** Panel (A) shows the predicted versus observed relative damage ( $R^2 = 0.189$ ) with a subpar performance. The data set is characterized by several extreme outliers, with up to 80% damage in selected forest districts. Panel (B) exhibits the feature importance of the independent variables.



#### 4.2.2 Identification of similar climatological regions based on Bioclim

The determination of climatic similarities was carried out in the course of this project for the growth area Mühl- und Waldviertel, where large-scale bark beetle calamities and thus an increase in damaged wood have occurred in recent years. In the following, the results for the target region Mühl- und Waldviertel are presented, subdivided into 20-year periods for the four scenarios (SSP1-26, SSP2-45, SSP3-70 and SSP5-85). For the purpose of brevity and clarity, only the most realistic scenario from the current perspective, SSP3-70, is shown for the considered time periods (Figures 20 to 23).

Since there are several realizations for the future data in Europe, the above analyses were calculated for the entire ensemble. Graphs were generated for the 0.1 quantile, the median (0.5 quantile) and the 0.9 quantile of the resulting distribution. In the following, only the plots of the medians are presented for the purpose of clarity.

##### 4.2.2.1 2021 - 2040

Similar climatological regions for growing area Mühl- und Waldviertel  
Quantil: 0.5

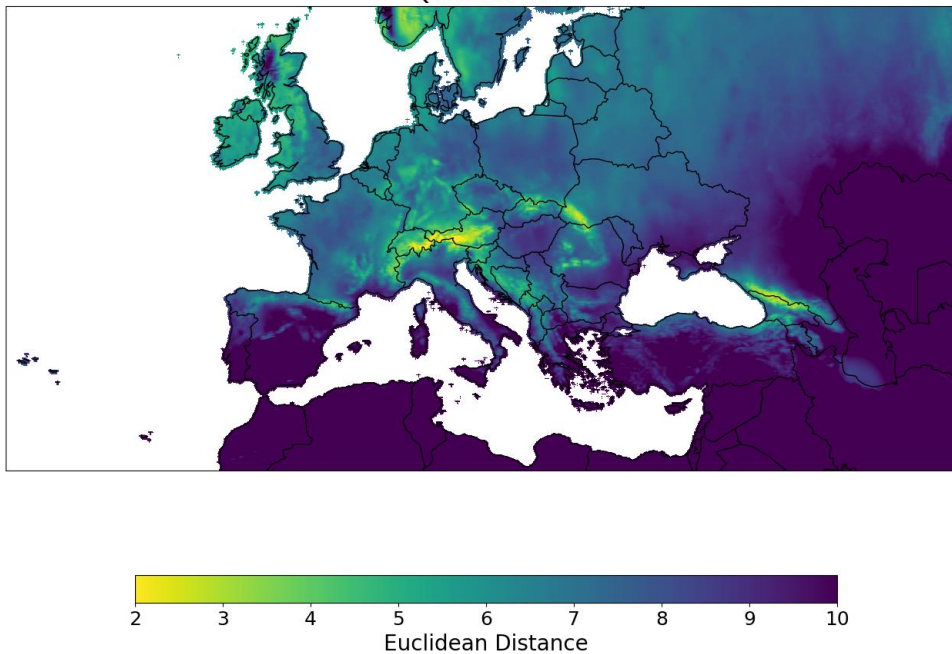


**Figure 20: Identification of regions that expect similar climatological conditions in the future (2021-2040; ensemble median) as have been observed in the target region Mühl- und Waldviertel in the past (1970 – 2000) considering the scenario SSP3-70. Yellow areas indicate values of low Euclidean distance or high similarity.**

#### 4.2.2.2 2041 - 2060

Similar climatological regions for growing area Mühl- und Waldviertel  
Quantil: 0.5

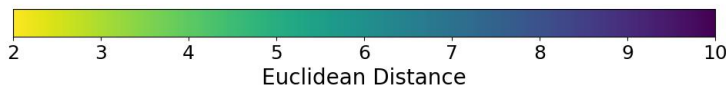
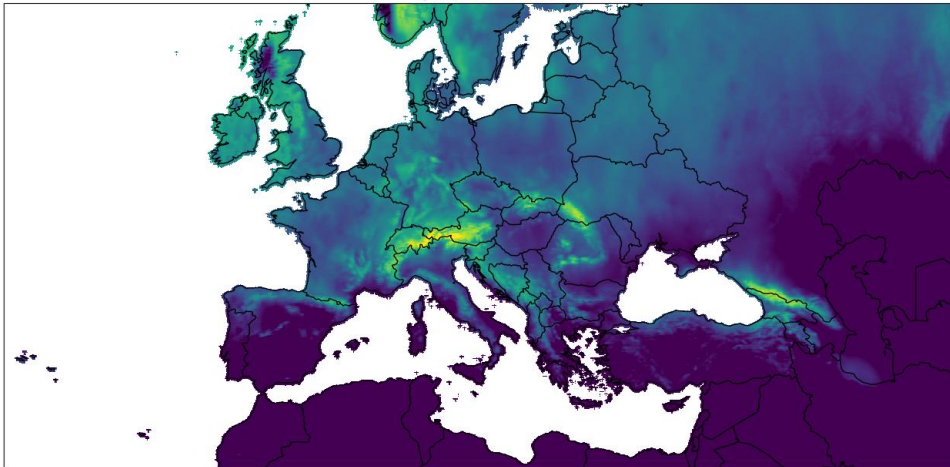


Figure 21: Identification of regions that expect similar climatological conditions in the future (2041-2060; ensemble median) as have been observed in the target region Mühl- und Waldviertel in the past (1970 – 2000) considering the scenario SSP3-70. Yellow areas indicate values of low Euclidean distance or high similarity.

#### 4.2.2.3 2061 – 2080

Similar climatological regions for growing area Mühl- und Waldviertel  
Quantil: 0.5

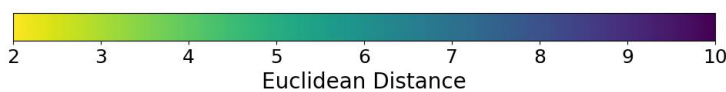
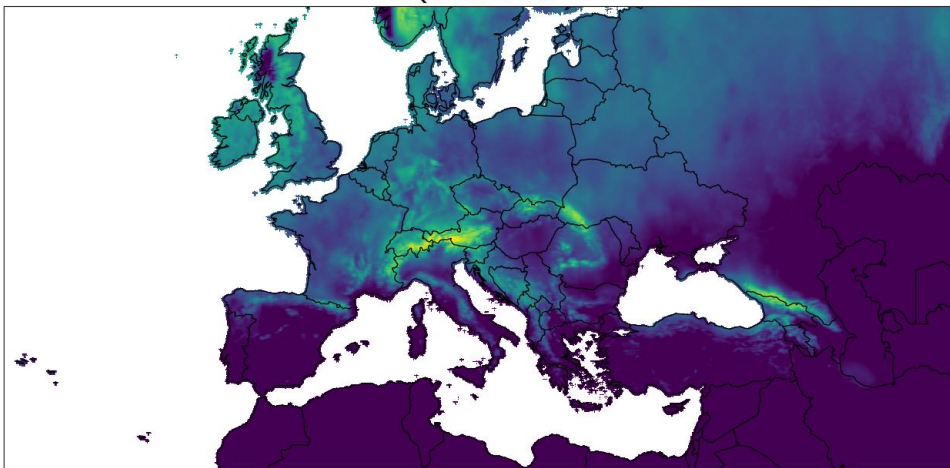
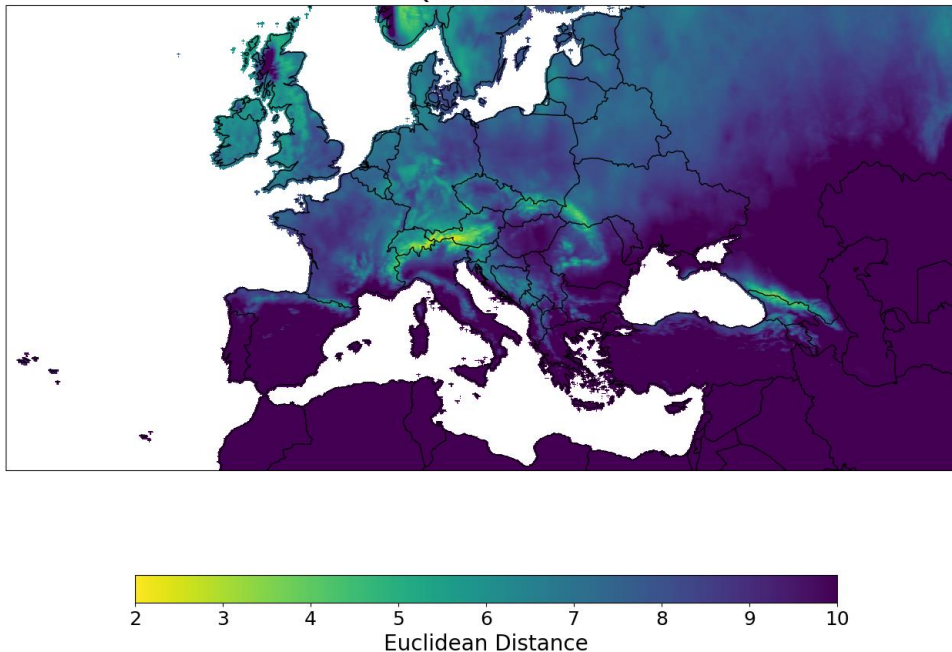


Figure 22: Identification of regions that expect similar climatological conditions in the future (2061-2080; ensemble median) as have been observed in the target region Mühl- und Waldviertel in the past (1970 – 2000) considering the scenario SSP3-70. Yellow areas indicate values of low Euclidean distance or high similarity.

#### 4.2.2.4 2081 – 2100

Similar climatological regions for growing area Mühl- und Waldviertel  
Quantil: 0.5



**Figure 23: Identification of regions that expect similar climatological conditions in the future (2081-2100; ensemble median) as have been observed in the target region Mühl- und Waldviertel in the past (1970 – 2000) considering the scenario SSP3-70. Yellow areas indicate values of low Euclidean distance or high similarity.**

#### 4.2.2.5 Discussion

In the time periods of the near future, there are hardly any differences between the different scenarios. This behaviour is to be expected due to the inertia of the climate system: different values of the additional radiative forcing show their effect only from the second half of the century. The same applies to the 19 bioclimatic variables considered. These show similar regions in the periods 2021- 2040 as well as 2041 - 2060 throughout the European Alpine region (Western Austria, Switzerland, Southeastern France) as well as in the Carpathians (Slovakia, Romania, eastern Ukraine, parts of Bulgaria) and east of the Black Sea (Southern Russia, Georgia, Azerbaijan, Armenia, and the Northeast of Iran).

The climate-friendly scenario SSP1-26 and the intermediate scenario SSP2-45 (both not shown here, see Appendix) assume nearly constant conditions in the near and far future. The scenarios SSP3-70 and SSP5-85 still consider large parts of the European mountain regions (Alpine region, Carpathians and Caucasus) as similar in the near future, the center of smallest Euclidean distance shifts more and more to higher altitudes in the distant future.

It has to be stressed that both the climatic similarity and the damage models are based on well-established bioclimatic indicators only. Eleven of these bioclimatic indicators relate to temperature, eight bioclimatic indicators relate to precipitation. These entails several limitations. The temperature and precipitation indicators do only reflect temperature and precipitation as major parameters. Information on other potentially important parameters, such as e.g. wind or snow damage caused by weight of snow are not covered. In addition, the bioclimatic variables are not independent. The presence of multicollinearity was not considered, which may lead to a slight bias (i.e. too much weight on temperature) in the similarity computations, as well as incorrect importance measures in the damage models.



#### 4.2.3 Identification of similar climatological regions based on ECLIPS2.0

The determination of climatic similarities was carried out in the course of this project for the growth area Mühl- und Waldviertel, where large-scale bark beetle calamities and thus an increase in damaged wood have occurred in recent years. In the following, the results for the target region Mühl- und Waldviertel are presented, subdivided into 20-year periods for the two scenarios (RCP4.5 and RCP8.5). For the purpose of brevity and clarity, only the results for the far future period (2081 until 2100) for both scenarios are exhibited in Figures 24 and 25.

Since there are several realizations for the future data in Europe, the above analyses were calculated for the entire ensemble. Graphs were generated for the 0.1 quantile, the median (0.5 quantile) and the 0.9 quantile of the resulting distribution. In the following, only the plots of the medians are presented.

##### 4.2.3.1 RCP4.5

Similar climatological regions for growing area Mühl- und Waldviertel  
Quantil: 0.5

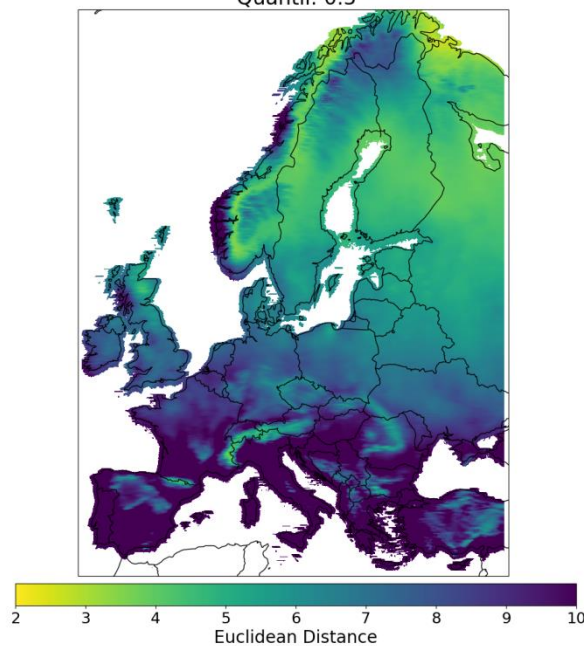


**Figure 24: Identification of regions that expect similar climatological conditions in the future (2081-2100; ensemble median) as have been observed in the target region Mühl- und Waldviertel in the past (1991 – 2010) considering the scenario RCP4.5 based on the first two principle components of the ECLIPS2.0 dataset.**

#### 4.2.3.2 RCP8.5

Similar climatological regions for growing area Mühl- und Waldviertel  
Quantil: 0.5

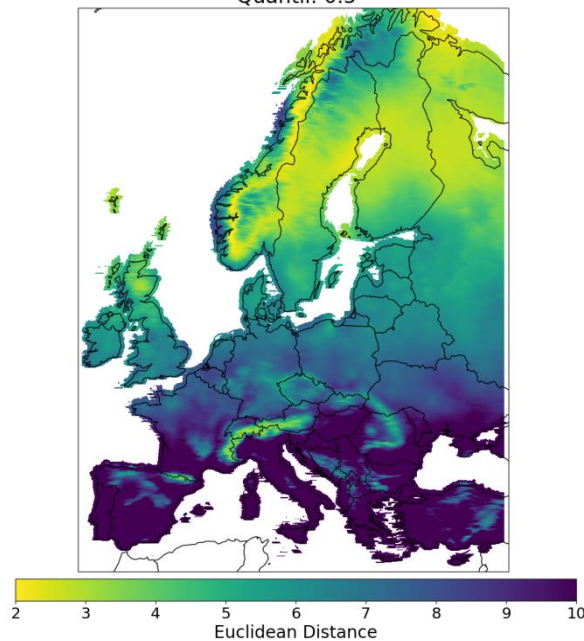


**Figure 25: Identification of regions that expect similar climatological conditions in the future (2081-2100; ensemble median) as have been observed in the target region Mühl- und Waldviertel in the past (1991 – 2010) considering the scenario RCP4.5 based on the first two principle components off he ECLIPS2.0 dataset.**

#### 4.2.3.3 Discussion

When calculating similar regions based on ECLIPS2.0 data dimensionally reduced with a principal component analysis, large parts of Northern and Eastern Europe as well as the European mountainous regions show high similarity values for both scenarios, whereas the pessimistic scenario RCP8.5 exhibits values of smaller Euclidean distance for these regions. The high similarity values in Scandinavia are particularly striking, although there is a high degree of regional variation. The influence of the Scandinavian mountains shielding precipitation induced by westerly airflows from the Atlantic Ocean is illustrated by the small band of high values of Euclidean distance along the Norwegian coastline. Beyond that mountain range, similarity exhibits higher values.

##### *Differences between the both approaches*

Both approaches are based on the same methodology – the calculation of the Euclidean distance between a past vector in the target region, and future vectors for each box over Europe. Nevertheless, results reveal substantial differences. The results using the 19-dimensional Bioclim variables show a clear shift from areas of potential future forestry importance to higher elevation areas. This is due to the fact that the majority of comprised bioclimatic variables are temperature dependent. The results show the (too) strong influence of temperature, which correlates highly with altitude. In contrast, the results on the dimensionally reduced ECLIPS data show a shift to the North, where e.g. precipitation regimes prevailing in the region are also evident in the graphs (shielding of precipitation alongside the Western Norwegian shore). The use of PCA also has the elegant side effect that not all indicators are weighted equally, but rather subsumed in the respective PCs. While this makes the interpretation of relevant indicators more cumbersome, the quality of the overall result is benefits from this indirect weighting, since results are assumed to be more robust.

The similarity was calculated on the basis of past data covering a period with very favourable climatic conditions for spruce and pine cultivation in the Mühlviertel and Waldviertel regions. Thus, it can be assumed that identified regions represent those areas in Europe that exhibit climatic conditions in which spruce and pine, respectively, are viable under the scenarios considered and in the respective time periods. These areas are therefore potentially relevant for future spruce and pine cultivation in Europe.

It is particularly important to emphasize that the similarity analyses for the identification of potentially relevant growth areas in the future were carried out solely on the basis of climatological conditions. Other important influencing variables for tree growth, such as soil properties and geology, are not included in these results.

### 4.3 Risk analysis

#### 4.3.1 Definition of risk measures and stock changes

**Table 6: Definition of risk measures.**

Value	Meaning
Future species risk [%]	<p>Probability of failure for a given tree species, i.e. the likelihood that a species which occurs today within a given NUTS2 region is affected by climate change and might experience losses until the end of the century. High values show high likelihood of failure, low values show low likelihood of failure.</p> <p>The future risk is calculated for single species and for multiple species.</p>
Stock Risk total [mill. m <sup>3</sup> ]	<p>Total current forest stock within a NUTS2 region that is threatened by the future probability of failure.</p> <p>The stock risk is given for single tree species and for the growing stock of all three tree species considered.</p>
Stock Risk average [m <sup>3</sup> /ha]	<p>Current average forest stock per ha within a NUTS2 region that is threatened by the future probability of failure. e.g. low standing stocks of given species result in low risk even if the species shows a high risk in climate change but high standing stock might result in high risk if the future species risk is high</p> <p>The stock risk is given for single tree species and for the growing stock of all three tree species considered.</p>
Potential future stock total [mill. m <sup>3</sup> ]	<p>Expected total future forest stocks within a NUTS2 region with changing probability of occurrence under future climate.</p> <p>The potential future stock is given for single tree species, for the two conifer species and for all three tree species.</p>
Potential future stock average [m <sup>3</sup> /ha]	<p>Expected forest stocks in future per ha given as average of a specific NUTS2 region on basis of a changing probability of occurrence under future climate.</p> <p>The potential future stock per ha is given for single tree species, for the two conifer species and for all three tree species.</p>
Stock change total [mill. m <sup>3</sup> ]	<p>Potential change of forest stocks as difference between current stocks and potential forest stocks in future within a specific NUTS2 region on basis of a changing probability of occurrence under future climate.</p> <p>The stock change total is given for single tree species, for the two conifer species and for all three tree species.</p>

Stock change average [m <sup>3</sup> /ha]	<p>Potential change of forest stocks as difference between current stocks and potential forest stocks in future per ha given as average of a specific NUTS2 region on basis of a changing probability of occurrence under future climate.</p> <p>The average stock change is given for single tree species, for the two conifer species and for all three tree species.</p>
Stock change [%]	<p>Potential change of forest stocks as percent calculated between current stocks and potential future forest stocks within a specific NUTS2 region.</p> <p>The stock change is given for single tree species, for the two conifer species and for all three tree species.</p>

### 4.3.2 Risk Maps

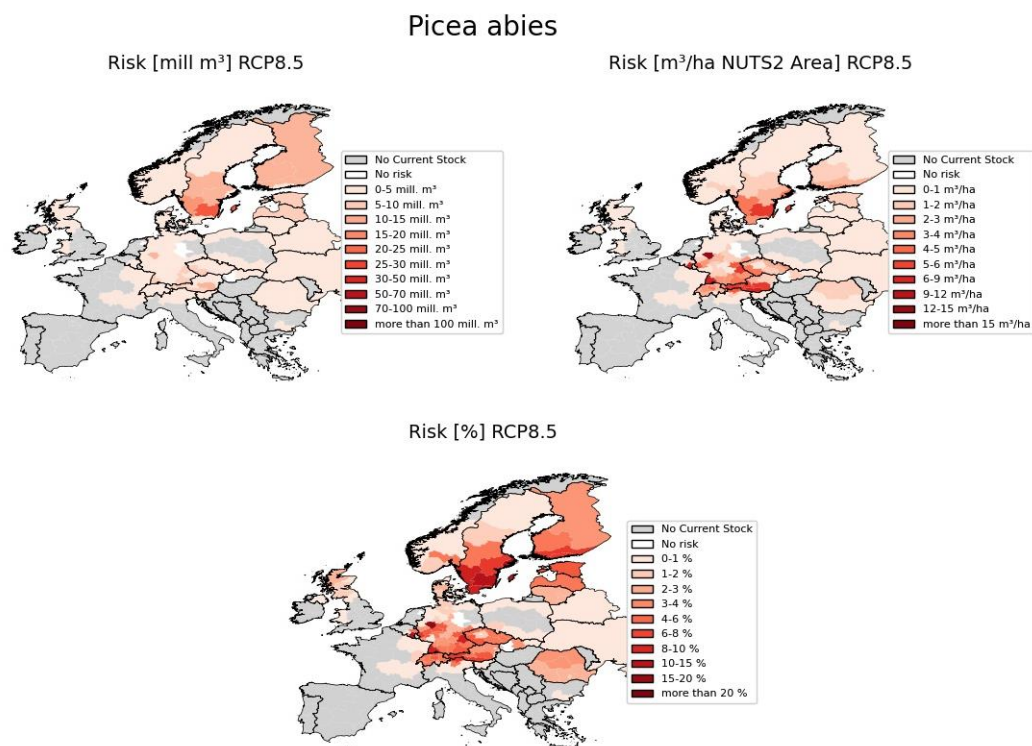


**Figure 26: Risk measures for *Picea abies* stocks for the period 2081-2100 predicted under the RCP8.5 climate change scenario for each NUTS2 region.**

The highest risk for Norway spruce forests, i.e. their probability of failure, can be found in Austria, Southern Germany, Switzerland, and the Czech Republic as well as in Southern Sweden and Southern Finland. Total stock risks, however, are highest in Southern Sweden and Finland. Taking the size of the NUTS2 areas into account, the average stock risks per ha values show highest risks in the alpine regions of Austria, Southern Germany, Switzerland, and the Czech Republic (Fig. 26).

For Scots pine forests, the highest species risks can be found in Finland, Eastern Poland, but also in Southeastern France. Total stock risks are at highest in Finland. Taking the size of the NUTS2 areas into account, the average stock risk values in Finland decrease and again a higher risk in Eastern Poland can be observed (Fig. 27).

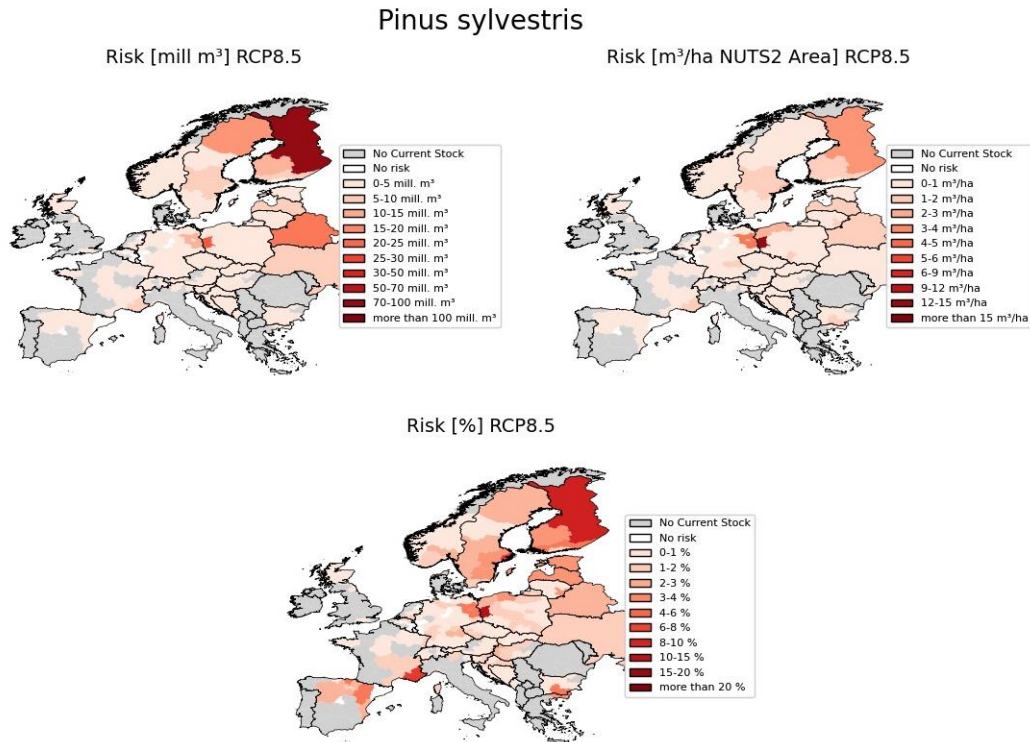


**Figure 27:** Risk measures for *Pinus sylvestris* stocks for the period 2081-2100 predicted under the RCP8.5 climate scenario for each NUTS2 region.

Under the current distribution of both coniferous species, *Picea abies* and *Pinus sylvestris*, the highest risk can be found in regions of Finland, Sweden and Belarus. Taking the size of the NUTS2 areas into account, the highest risk of stocks per ha is currently in Austria, Southern Germany and parts of Poland. (Fig. 28).

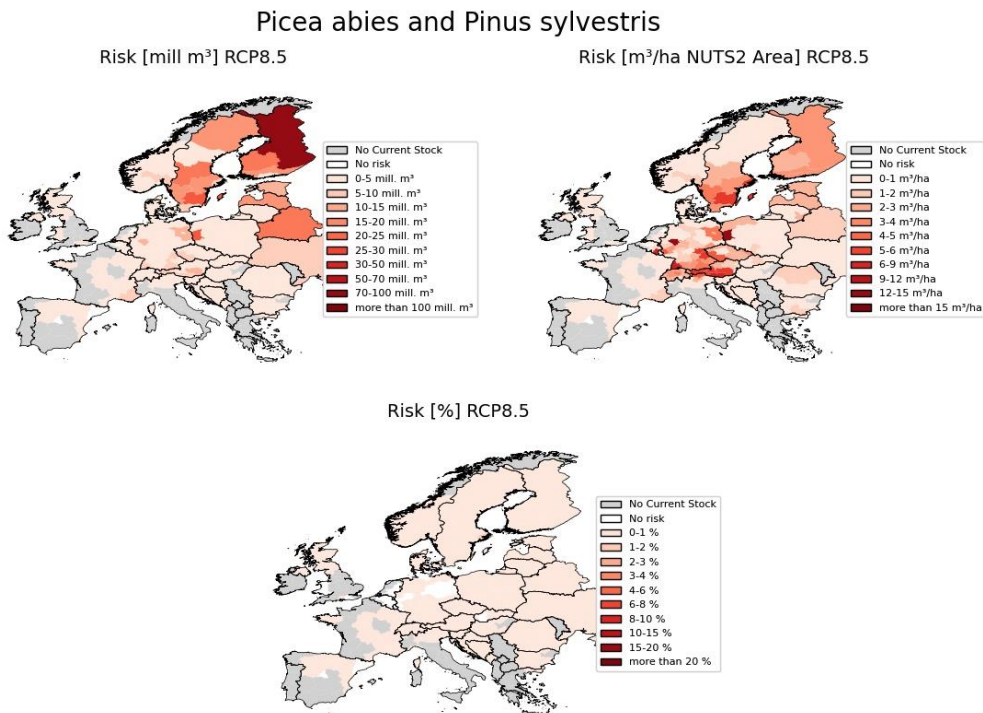


**Figure 28:** Risk measures for *Pinus sylvestris* and *Picea abies* stocks for the period 2081-2100 predicted under the RCP8.5 climate scenario for each NUTS2 region.



For European beech, the future species risk was found to be highest in Southern Europe, namely in Bosnia-Herzegovina and Slovenia. Also the total stock risk is highest in Bosnia-Herzegovina, and the average stocks risks again in Slovenia and Bosnia-Herzegovina (Fig. 29).

The combined future species risk, i.e. the probability of failure of all species together is generally lower as for single species and low all across Europe. Especially Northern Europe shows very little future risks (Fig. 30). However, Northern European forests and the growing stocks here are mainly composed of the conifers Scots pine and Norway spruce, while the share of these species is lower in Central and Southern Europe. Thus, the total stock risks are at highest in Northern and Eastern Europe. Taking the size of the NUTS2 areas into account, the average stock risk is highest in parts of Austria and Germany (Fig. 30).

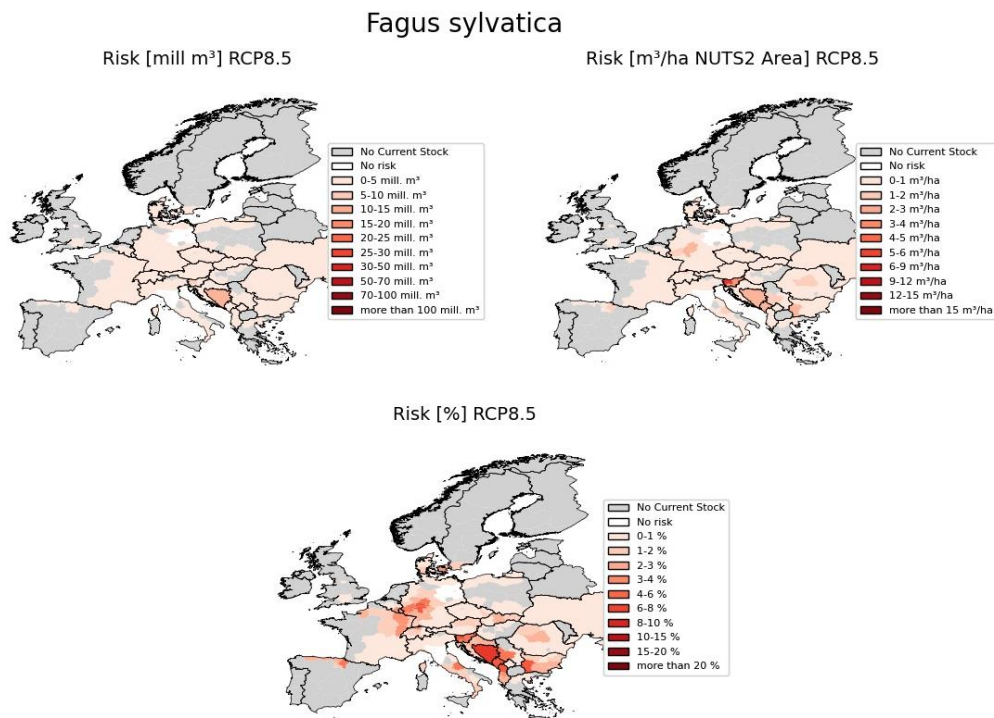


**Figure 29: Risk measures for *Fagus sylvatica* stocks for the period 2081-2100 predicted under the RCP8.5 climate change scenario for each NUTS2 region.**

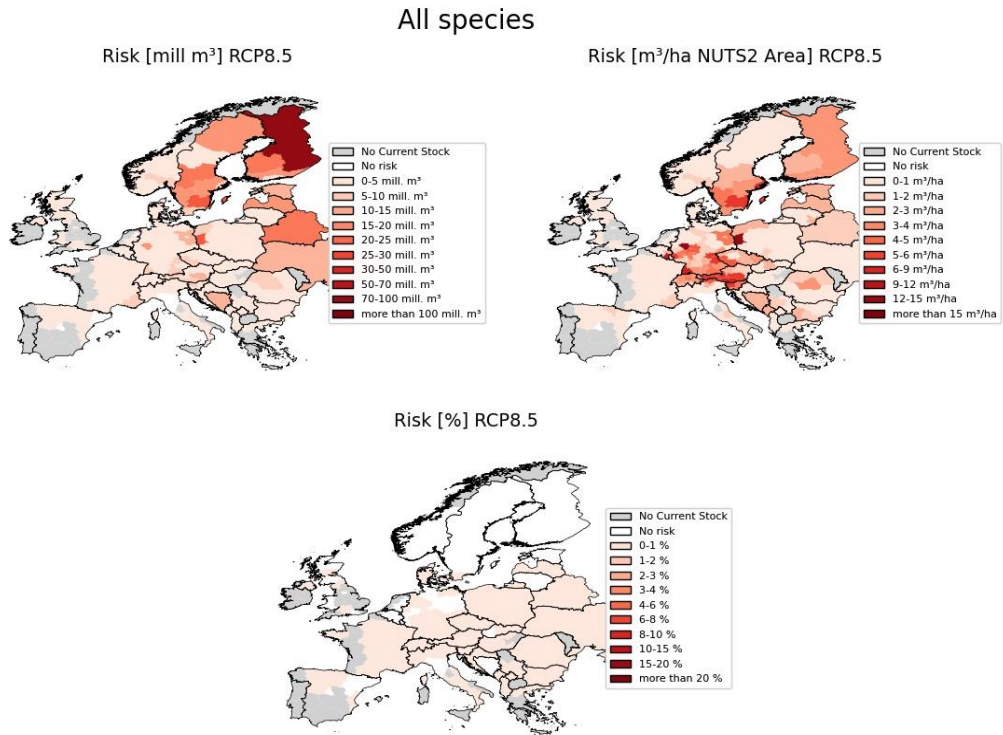


Figure 30: Risk measures for all species (*Picea abies*, *Pinus sylvestris* and *Fagus sylvatica*) and their growing stocks for the period 2081-2100 predicted under the RCP8.5 climate change scenario for each NUTS2 region.

### 4.3.3 Current and potential future stocks

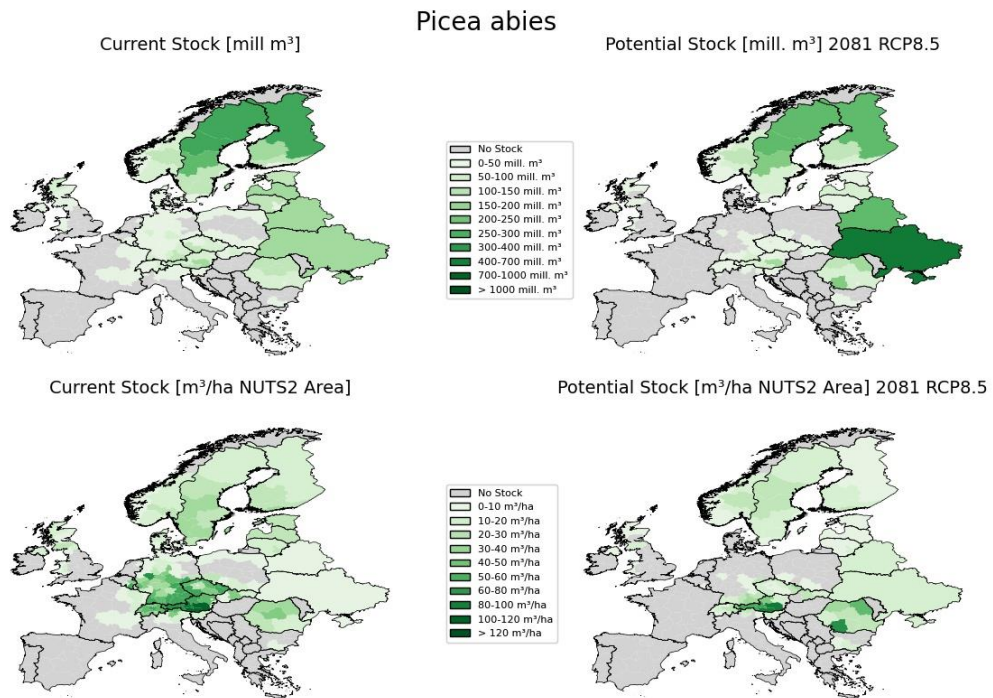
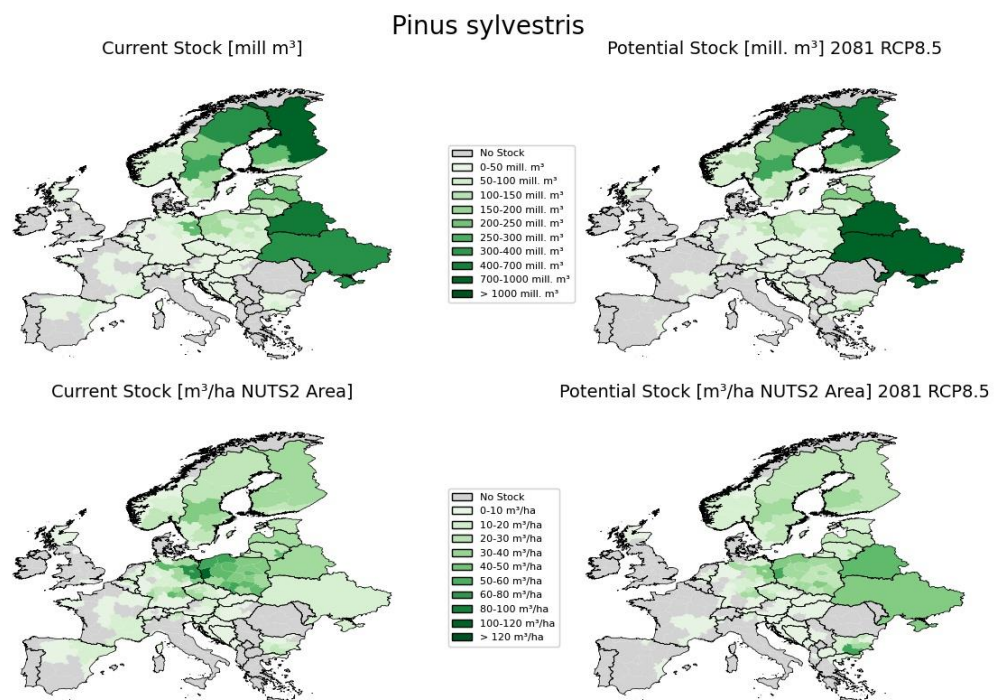


Figure 31: Comparison of current stocks of *Picea abies* and predicted potential future stocks for the period from 2081 to 2100 under the RCP8.5 climate scenario for each NUTS2 area.

The current distribution of *Picea abies* shows the highest total stock values in NUTS2 regions of Sweden and Finland. The predicted future total stocks indicate a reduction in Sweden and Finland and an increase in Belarus and the Ukraine, where the stocks are predicted to be highest. Due to the declining distribution in France and Germany, potential stocks here are expected to decline. Taking into account the size of the NUTS2 areas, the stocks per ha are currently highest in Austria, Switzerland, Southern Germany, and the Czech Republic. These stocks are expected to decrease but may remain mainly in the Alpine area and shift mainly to the alpine regions in Austria as well as in Romania (Fig. 31).

Currently, the highest total stocks of Scots pine can be found in Finland, Belarus and the Ukraine and the highest average stocks per ha Poland and Eastern Germany. The predicted total future stock show only little changes in Northern and Eastern Europe but the stocks will decrease and disappear in Northern Spain and parts of France (Fig. 32).

Under the current distribution of both coniferous species, *Picea abies* and *Pinus sylvestris*, the highest total stocks can be found in regions of Sweden, Finland, Belarus and the Ukraine. The potential total future stocks will stay highest in these Northern and Eastern Europe, but large parts of the current stocks in France and Spain will be lost. Taking the size of the NUTS2 areas into account, the stocks per ha are currently highest in Austria, Southern Germany, the Czech Republic, and Poland. These stocks decrease and highest values of potential future stocks are stated in Belarus and the Ukraine (Fig. 33).



**Figure 32: Comparison of current stocks of *Pinus sylvestris* and predicted potential future stocks for the period from 2081 to 2100 under the RCP8.5 climate scenario for each NUTS2 area.**



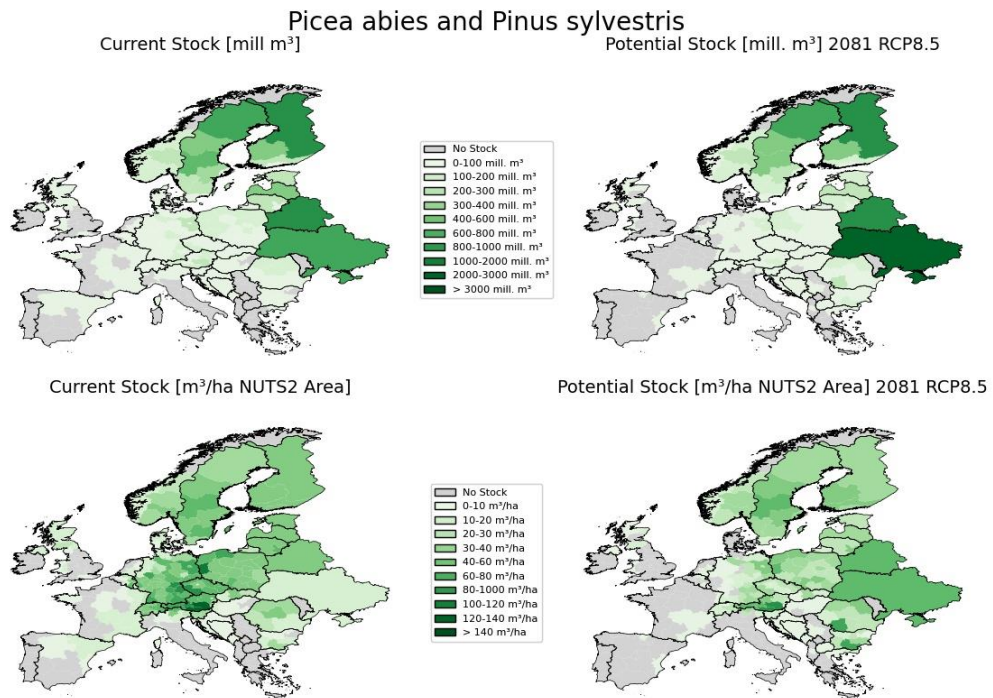


**Figure 33: Comparison of current stocks of conifers (*Picea abies* and *Pinus sylvestris*) and predicted potential stocks for the period from 2081 to 2100 under the RCP8.5 climate scenario for each NUTS2 area.**

European beech shows highest total values under current conditions in the Ukraine. The potential future total stocks might even increase in this area, while large parts in France, Northeastern Germany, and Czech Republic will lose beech stocks. Taking into account the size of the NUTS2 areas, the stocks per ha are currently and in future at highest in Slovenia and Romania (Fig. 34).

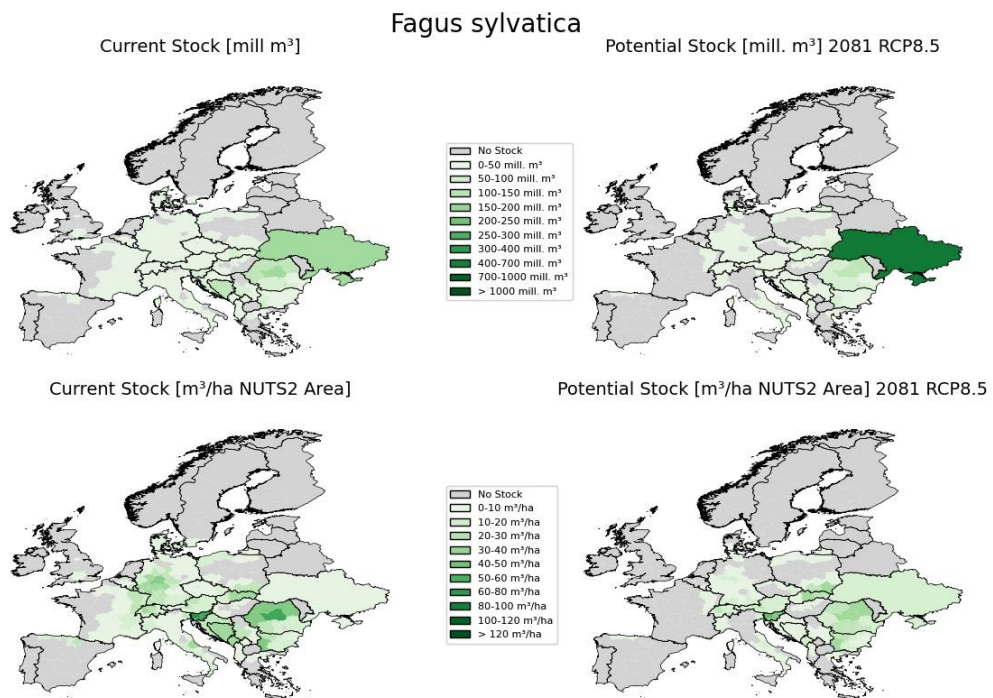


**Figure 34: Comparison of current stocks of *Fagus sylvatica* and predicted potential future stocks for the period from 2081 to 2100 under the RCP8.5 climate scenario for each NUTS2 area.**

Currently, the highest total stocks of the three species can be found in Ukraine, Belarus, and Finland. The predicted future total stocks show no change in the distribution of the highest stocks but overall decreases especially in Spain, France, and Italy. Taking into account the size of the NUTS2 areas, the stocks per ha are currently highest in Austria, Switzerland, Southern Germany, and the Czech Republic. These stocks are expected to decrease. Higher stocks might in the future be expected in Eastern Europe, i.e. Belarus, the Ukraine, and Romania (Fig. 35).

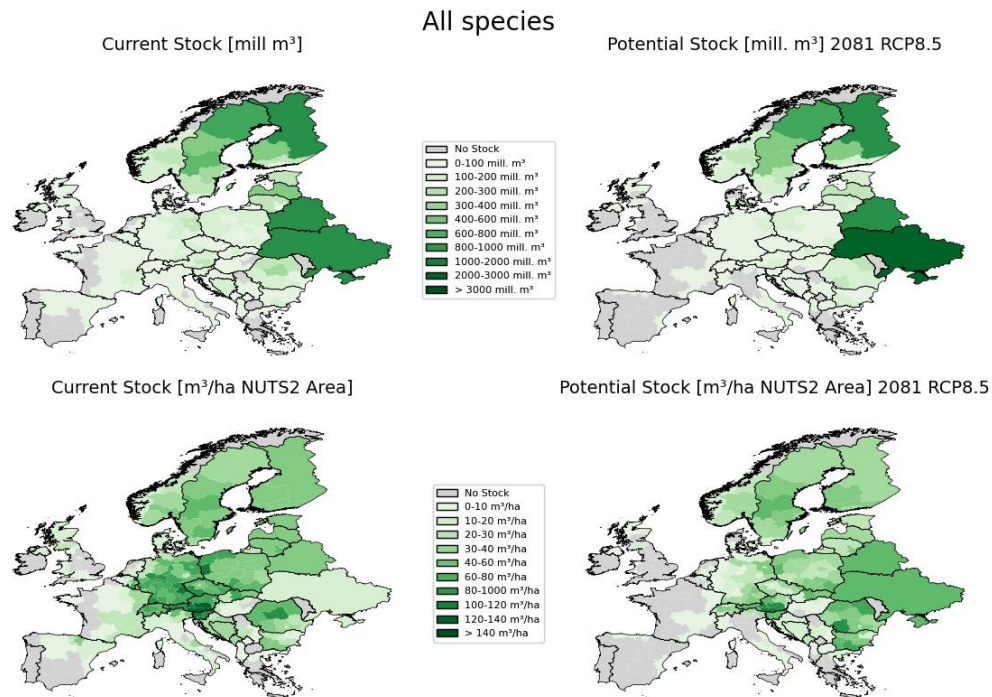


**Figure 35: Comparison of current stocks of all three species (*Picea abies*, *Pinus sylvestris* and *Fagus sylvatica*) and predicted potential future stocks for the period from 2081 to 2100 under the RCP8.5 climate scenario for each NUTS2 area.**

#### 4.3.4 Stock changes

Total values of stocks of Norway spruce will decrease in the whole distribution area, except in the Ukraine, Belarus, and Romania. The highest negative average stock change per ha is predicted to be highest in Southern Germany, Austria, Switzerland, and the Czech Republic, while the highest positive stock change can be found in the Ukraine and Belarus. In relation to the current stocks, the stock change in Germany, Austria, Switzerland, and the Czech Republic is even more impressive as it may reach up to -100% in some Central European NUTS2 regions (Fig. 36).

The strongest stock change for Scots pine (*Pinus sylvestris*) is expected in Northern and Western Europe. In contrast, Belarus and the Ukraine show the highest stock increase, but also in Southeastern Europe a stock increase can be observed. Taking the size of the NUTS2 areas into account, stock changes per ha show similar geographic patterns. In relation to the current stock, the stock loss in Spain, France, Germany, and Eastern Europe is strongest and reaches up to 100% (Fig. 37).

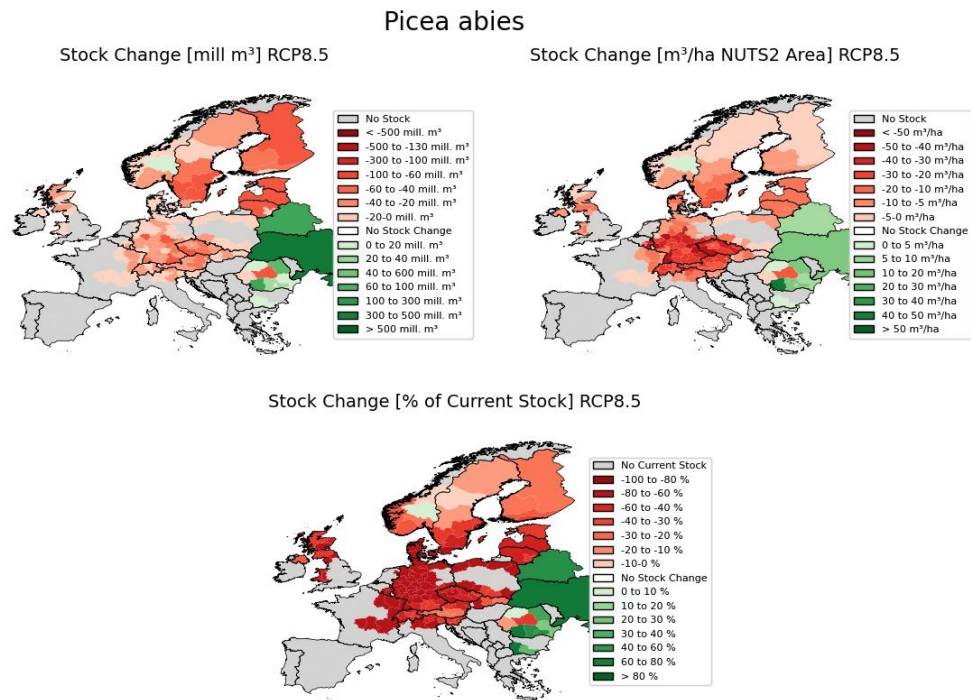


**Figure 36: Stock changes of *Picea abies* from current to potential future stocks for the period from 2081 to 2100, predicted under the RCP8.5 climate scenario for each NUTS2 area.**

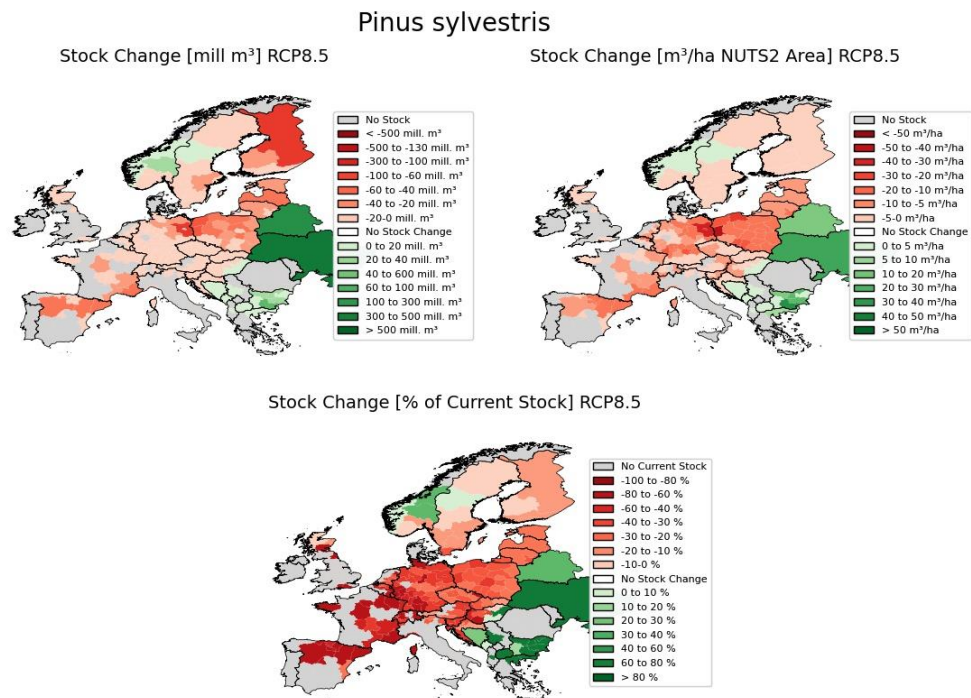


**Figure 37: Stock changes of *Pinus sylvestris* from current to potential future stocks for the period from 2081 to 2100, predicted under the RCP8.5 climate scenario for each NUTS2 area.**

The combined forest stocks of the two conifers will undergo declines nearly throughout Europe, except in the Ukraine, Belarus, and Southeastern Europe. The highest stock reductions are predicted for Finland, Estonia, Latvia, and Lithuania. The highest average losses per ha are in Central Europe (Southern Germany, Austria, Czech Republic). The highest percent change of stocks is expected in Central and Southwestern Europe as well as in the North of Great Britain (Fig. 38).



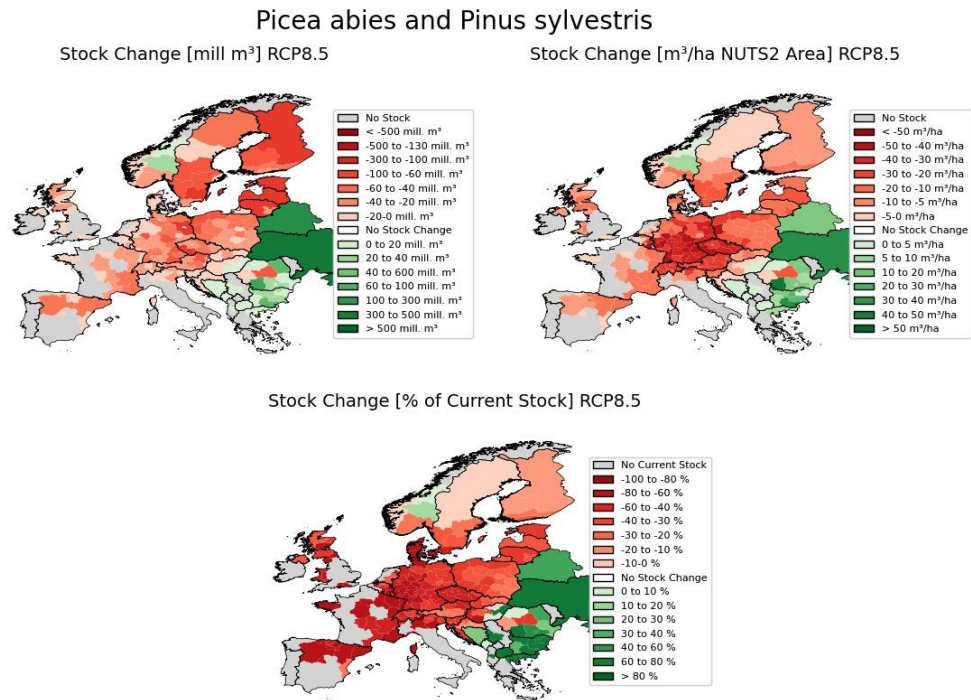


**Figure 38: Stock changes of coniferous species (*Picea abies* and *Pinus sylvestris*) from current to potential stocks for the period from 2081 to 2100, predicted under the RCP8.5 climate scenario for each NUTS2 area.**

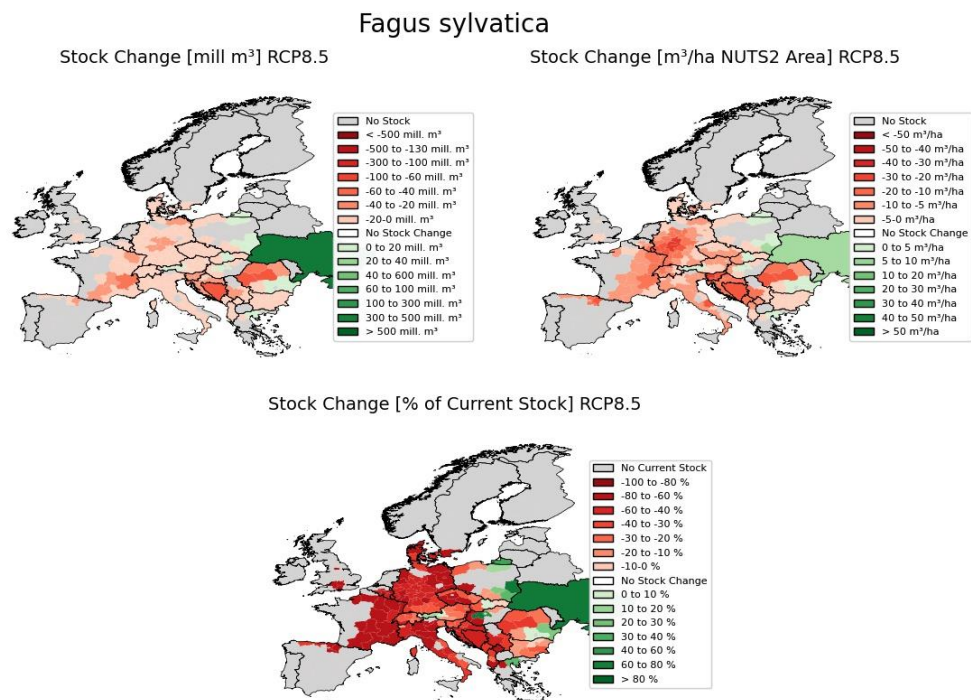


**Figure 39: Stock changes of *Fagus sylvatica* from current to potential future stocks for the period from 2081 to 2100, predicted under the RCP8.5 climate scenario for each NUTS2 area.**

Absolute values of stocks of *Fagus sylvatica* will decrease in the whole distribution area, except in the Ukraine and small parts of Austria and Eastern Europe. Taking the size of the NUTS2 areas into account, the values per ha show the same shift but put into perspective the high stock increase in Ukraine. The dramatic loss of stocks in Germany, France, and Southern Europe is even more impressive taking into account the relation to the current stocks (Fig. 39).

Absolute stock changes for all three tree species are negative nearly across Europe, except for Ukraine, Belarus, and parts of Southeastern Europe. Taking the size of the NUTS2 areas into account, the average change per ha is similarly negative but shows the strongest decline in Southern Germany, Austria, Switzerland, and the Czech Republic, and puts into perspective the stock increase in Ukraine and Belarus. In relation to the current stocks, the predicted stock losses in Central and Southwestern Europe and parts of the UK are immense (Fig. 40).

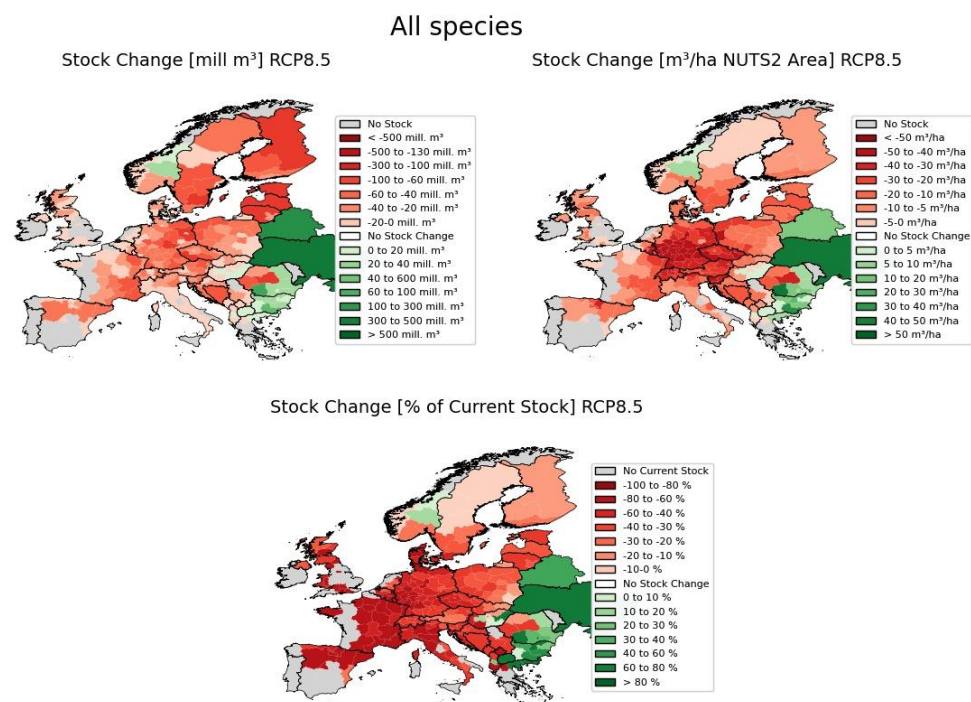


**Figure 40: Stock changes of all species (*Picea abies*, *Pinus sylvestris* and *Fagus sylvatica*) from current to potential stocks for the period from 2081 to 2100, predicted under the RCP8.5 climate scenario for each NUTS2 area.**

## 5 Conclusion

Climate change presents a major challenge for forest management as well as for wood-based industries. Besides expected long-term changes of wood assortments due to the shifts in the tree species distribution under changing conditions, also an increasing frequency of disturbances by wind, drought, and or other weather-related events can be expected, which might often be accompanied by bark-beetle calamities. The present study aimed at identifying risks for forest stocks and expected stock changes until the end of the century as basis for feedstock availability. We used several datasets for our study:

1. Europe-wide data on growing stock estimated by remote-sensing which were evaluated regionally by terrestrial forest inventory information
2. Europe-wide data on growing stock on national level provided by country-specific institutions for international statistics
3. Europe-wide data on current species shares
4. Europe-wide models of tree species suitability under current climate and expected climate change scenarios
5. Two datasets of climate data in a resolution of 1 x 1km as basis for identifying regions that are climatically similar to two target regions in Austria that have been among the most productive forest regions by the end of the 20th century.

These five datasets have been combined to evaluate the geographical distribution of current growing stocks of Scots pine and Norway spruce, which are the two most important European conifers as well as of European beech, the most important deciduous tree species. Moreover, we analyzed climate extremes and identified climatic drivers of forest damage agents. Finally, we calculated the climate risk of the three selected tree species and of their growing stocks and estimated potential future stocks and stock changes in climate change.

A major challenge of the present study and many other transnational projects is the availability, respectively non-availability of fully harmonized data in Europe. This is because National Forest Inventories differ from country to country in terms of definitions, methodology, and observation periods. Therefore, for the present analysis, we used rasterized forest stock estimates that were derived from remote sensing data and compared them with terrestrial inventory data from the National Forest Inventory of Austria. This comparison revealed a moderate overestimation of growing stocks using remote sensing data. However, it can be explained by the inaccessibility of several protective forest areas in the Austrian Alps which are not assessed by the terrestrial inventory, but quantified by remote sensing approaches. Correcting the terrestrial inventory data with inaccessible sites resulted in highly comparable growing stocks across the Austrian NUTS2 regions. This high correspondence supports the utilization of remote sensing estimates also for calculations of growing stocks across Europe.

Overall, the estimated distribution of current growing stocks corresponds well with other maps by Verkerk et al. (2015) and Verkerk et al. (2019) derived from other forest data sources. For example, Verkerk et al. (2015) used sets of biophysical and socioeconomic factors as well as wood production statistics between 2000 to 2010 from 29 European countries to produce maps indicating the wood harvests on a 1 x 1 km<sup>2</sup> grid (see Fig. 41). The highest harvest likelihood has been identified in Central Europe and the Southern part of Northern Europe and compares with the growing stock distribution of our study. Other sites with high wood harvests (i.e. Southwestern France) do not concern any of the three tree species studied here. In another study, Verkerk et al. (2019) applied international forest statistics and the European Forest Information Scenario model to estimate the theoretical average amount of biomass that could be available annually taking current and future development of forest age-structures, growing stock, increment and various environmental and technical conditions into accounts. The spatial distribution of this potential woody biomass availability resolved on NUTS2 Level and on average values per ha resulted in patterns (Fig. 42) very comparable to our remote sensing approach.



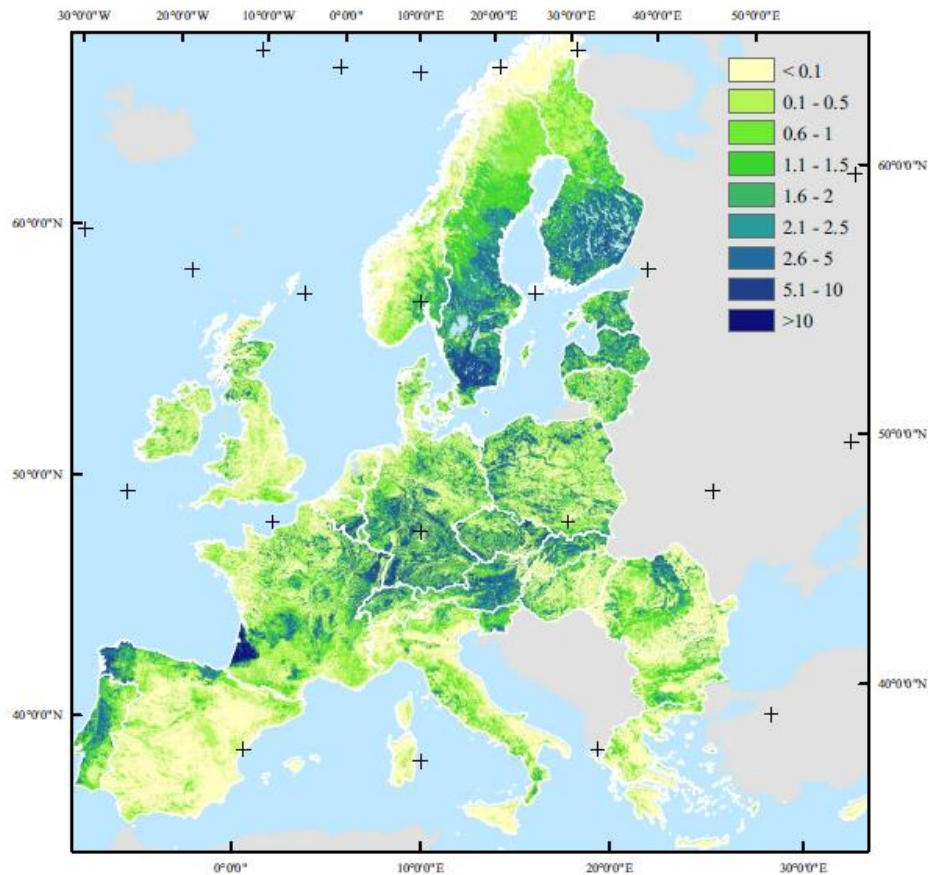


Figure 41. Map from Verkerk et al. (2015) showing predicted wood production [unit:  $\text{m}^3 \text{ha}^{-1} \text{land yr}^{-1}$ ] in Europe averaged over the period 2000–2010 by disaggregating statistics from administrative units to  $1 \times 1 \text{ km}^2$  raster maps with the linear model.

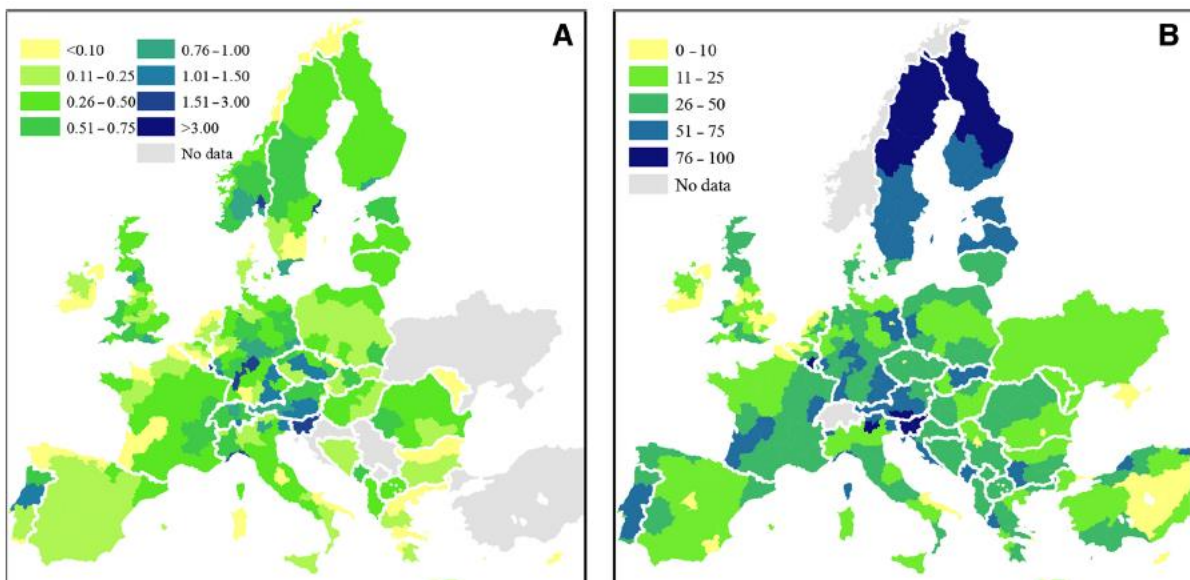


Figure 42. Maps from Verkerk et al. (2019): estimated forest biomass from availability according to the BASE potential (potential most closely aligned to current guidelines of sustainable forest management) at NUTS-2 level, expressed as unused potential per unit of land (A;  $\text{t} \cdot \text{ha}^{-1} \cdot \text{yr}^{-1}$ ) and as proportion of total ligno-cellulosic biomass potential in the region (B;  $\% \cdot \text{yr}^{-1}$ ).

Our study included a detailed assessment of forest mortality and damaged wood volumes in Austria, because we aimed at understanding immediate causes of forest dieback and reductions of forest stocks. The two most important drivers of forest damages in the Austrian database of forest damages have been bark beetle attacks (*Ips typographus*) and drought. Our analysis of climate and environmental variables that determine these forest mortality drivers identified a significant model only for bark beetle attacks. The most important climate variables have been the annual precipitation, the precipitation of the wettest (=summer) quarter and the temperature of the warmest (=summer) quarter. However, more important than the actual climate conditions have been the forest damages of the previous year, confirming that large scale disturbances by wind, drought, snow or ice break continue to be initiating events for bark beetle expansions and that the efficiency to manage damaged wood and remove breeding materials are main instruments for halting bark beetle degradations.

To evaluate potential changes of growing stocks, we used different risk metrics, all of which were based on tree species distribution maps, often also denoted as climate envelope models. These models are state-of-the-art tools to quantify the relationships between the present occurrence of tree species and their climate niche and consequently, to estimate future distribution under specific climate change scenarios.

The combination of tree species distribution models for the end of the century with current forest stocks can also be seen as a limitation of our study, as it is based on the assumption that present forest stocks will stay more or less constant for the next decades. This assumption is likely not true and depends on present forest age distributions, ongoing harvesting regimes and national and European policies. Within the last 70 years (more or less since the 1950ies) forest area and forest stock increased continuously and only within the last decade, first signs of stock (and carbon) saturation have been observed. It is thus not clear if the assumption of constant forest stocks is realistic for the next 50 years. A more accurate modeling study would need to take all these variables into account and should be based on empirical forest growth models.

The applied risk metrics can be grouped into two categories: first, we calculated the stock risk for a single species or group of species by considering current growing stocks and the likelihood that a species which occurs today within a given region is affected by climate change and might experience losses until the end of the century. Thus, the stock risk quantifies the growing stock that is threatened by the future climate conditions. Second, we calculated future stocks and stock changes by assuming a relationship between the probability of occurrence of a given species (in relation to climate) and their forest stocks. Our study did not allow for testing if the assumption of the latter relationship is true: at larger spatial scales, we can expect that it holds true because only trees that occur are available for cultivation and produce growing stocks. At local and regional scales, however, it might be confounded by the forest age structure, local disturbance pattern and forest management intensity. For example, intensive forest management including restrictive salvage cutting might support a productive forest management even at sites which are at the climatic limit of a given species (i.e. Norway spruce at low elevations). Therefore, we suggest considering both risk metrics for better understanding of the potential forest and stock development and stock risks, respectively.

Our risk metrics are given in relation to the stock of the complete region (NUTS2), as average stock per ha and as change in relation to the current stocks. Although based on the same data, these three references show different geographical patterns and should be interpreted differently. The total stock change of a complete region might be related to the demands of regional forest-based industries, i.e. to estimate if certain saw and paper mills may find enough feedstock in the future. In contrast, the average stock change per ha might rather be an important quantity for forest owners and land managers as it may help evaluate forest risks and the profitability of future stocks. Finally, stock change in relation to current stocks could be an interesting quantification for regional and national wood markets: with expected stock changes of 50% or more, national timber markets might be strongly disturbed resulting in a decline of investments and loss of industry and employment.

Generally, the different risk metrics show comparable geographical patterns. For example, the highest stock risks per ha were identified in Central Europe (AT, DE, CZ, SLO) and Southern Sweden. This is

comparable to the expected stock change, where also Central European countries (DE, AT, CH, CZ) were found to see the largest decline.

Interestingly, the risks for forest stocks in Western and Southwestern Europe are relatively small, but the expected stock change is among the highest across Europe and may reach up to 100%. This is because the current stocks of the three tree species here are relatively small and thus even with high climate risks only a small part of the overall stocks are concerned - and this small part is highly endangered under future conditions.

In contrast, the climate risks are relatively small in Northern European countries, but here the total stock risks are relatively high. This can be explained by the fact that forests in Northern countries are dominated by Norway spruce and Scots pine and this high share results in high risk values despite a lower risk probability. Also, due to the large size of the NUTS2 regions in Northern Europe, total stock risks are relatively high per region, but average stock risks per ha are mostly lower than in Central Europe.

An interesting observation can be made for Eastern Europe, namely for the Ukraine and Belarus. This region is the only region, where our stock calculations suggest an increase of forest stocks for all three tree species. However, this positive stock development should be interpreted very carefully, because it is not reflected by the respective stock risk measures (Fig. 30), that shows similar species and stock risks as in neighboring regions. The effect of positive stock development is only due to a moderate increase of climate-driven probability of occurrence mainly in the Western part of these countries as shown in Fig. 5. If these moderate increases of climate suitability for Norway spruce, Scots pine and beech will motivate land owners and managers to reforest with tree species that are considered high risk in the Eastern parts of their countries remains uncertain. Also, these predictions do not consider thresholds of species suitability above which long-term management for these species can be considered an economically interesting land use option.

Another confirmation for the obtained geographical distribution of forest risk comes from the modeling of climate similarities between the Austrian forest growth region 9: Mühl- and Waldviertel with other European regions. This purely climatic comparison aimed at identifying European regions which have relatively good climate condition for conifer production because the Mühl- and Waldviertel have been among the most productive conifer regions in the last decades of the 20<sup>th</sup> century and between 1990 and 2010. The comparison revealed comparable climate conditions by the end of the century across the Alps and the Carpathian mountain belt, but mainly across the Fennoscandian Peninsula approximately North of 60° latitude. Regions in the Ukraine and Belarus show very little climate similarities confirming the probably limited chances for conifer production here.

Aside from the present study, so far there are very few comparable attempts to predict forest stocks and stock risks under ongoing climate change and climate extreme events. This is mainly because past disturbance events rarely cover the extreme dieback scenarios that we observed in the last five years and even within the latest statistics, the damages between 2017 and 2020 are rather rare outliers. However, a full analysis of past disturbances confirms the geographical distribution of our predictions: Forzieri et al. (2021) analyzed climate-driven forest disturbance events across Europe between 1979 and 2018 using disturbance data and satellite images and showed that within the 39 years up to 33.4 billion tonnes of biomass have been affected. The hotspots of these disturbances which included windthrows (storms), fires and insect outbreaks were mostly found at the climate limits of the respective species envelopes. This confirms our approach to use climate-driven species distribution models (=climate envelopes) to define climate risks for individual species. Figure 43 shows the spatial distribution of past disturbance events. For the three species of our study, the relatively high disturbance index in the Alpine area and Fennoscandia are of interest. The high disturbance index in the Alpine area has been mainly caused by windthrows and insects outbreaks, while especially Eastern Fennoscandia showed high frequency of fires and insect outbreaks.

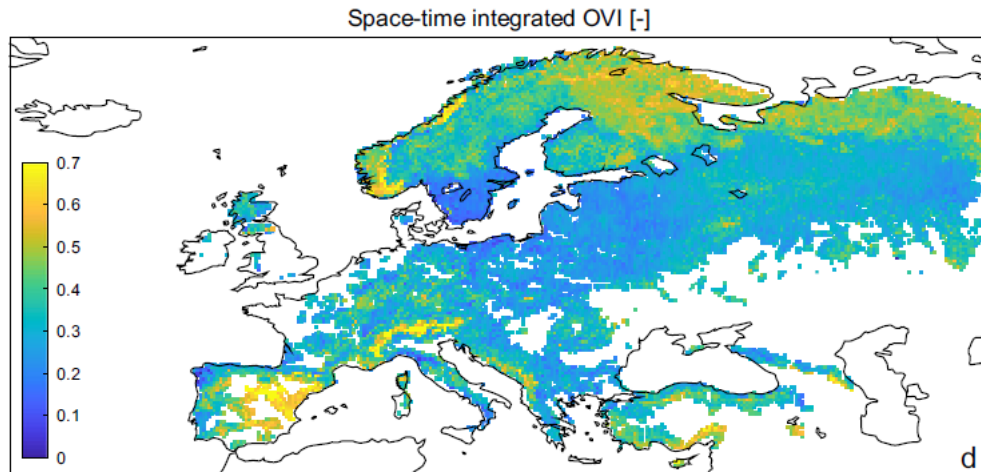


**Figure 43. Spatial patterns of the overall vulnerability index (OVI) of forests to multiple natural disturbances. Forests with cover fraction lower than 0.1 are masked in white**

Modelling and visualizing future forest development in climate change is of utmost importance for developing adaptation strategies for forest owners, policy makers and wood-based industries. However, modeling outcome needs to be interpreted carefully as each approach includes inherent assumptions and development scenarios. Our study was based on a certain climate change scenario which assumes a temperature increase between 2.7 and 6°C until the end of the century. So far, the uncertainty of our climate future provides the highest uncertainty to our study. Another limitation of our risk metrics is the uncertain time, when (until the end of the century) an extreme climate event may affect present forests and forest stocks. In addition, the future forest risks will also depend on the implementation of forest adaptation measures within European forests. These measures include more mixed and broadleaved species stands, better genetic material with resilience towards drought, shorter rotation periods and the harvesting of smaller wood assortments to reduce risks for windthrows, consequent thinning measures and forest protection measures. A consequent implementation of forest adaptation will likely reduce the risks of climate-induced calamities and cannot be fully considered in modeling predictions.



## 6 References

- Alberdi I., Bender S., Riedel T., Avitable V., Boriaud O., Bosela M., Camia A., Cañellas I., Castro Rego F., Fischer C., Freudenschuß A., Fridman J., Gasparini P., Gschwantner T., u.a. , 2020: Assessing forest availability for wood supply in Europe. *Forest Policy and Economics*, Amsterdam, 111(102032): open access
- Brus, D.J., Hengeveld, G.M., Walvoort, D.J.J., Goedhart, P.W., Heidema, A.H., Nabuurs, G.J., Gunia, K., (2011). Statistical mapping of tree species over Europe. *European Journal of Forest Research* 131 (1): 145–157.
- Brus, D. J. , Hengeveld, G. M., Walvoort, D. J. J., Goedhart, P. W., Heidema, A. H., Nabuurs G. J. & Gunia K., (2012). *European Journal of Forest Research* volume 131, pages 145–157. Available at: <https://doi.org/10.1007/s10342-011-0513-5>
- Chakraborty D, Matulla C, Andre K, Weissenbacher L, Schueler S (2019) Survival of Douglas-fir provenances in Austria: site-specific late and early frost events are more important than provenance origin. *Ann For Sci* 76: 100.
- Csilléry K, Kunstler G, Courbaud B, Allard D, Lassègues P, Haslinger K, Gardiner B (2017). Coupled effects of wind-storms and drought on tree mortality across 115 forest stands from the Western Alps and the Jura mountains. *Global Change Biology*. doi:10.1111/gcb.13773.
- Dyderski MK, Paź S, Frelich LE, Jagodziński AM (2018) How much does climate change threaten European forest tree species distributions? *Glob Change Biol* 24: 1150–1163
- FAO, 2020. *Global Forest Resources Assessment 2020 - Main report*. Food and Agriculture Organisation of the United Nations, Rome, 164 p.
- Fick, S.E. and Hijmans, R.J., 2017. WorldClim 2: new 1-km spatial resolution climate surfaces for global land areas. *International Journal of Climatology*, 37(12), pp.4302–4315. Available at: <https://doi.org/10.1002/joc.5086>
- Gschwantner et al. (2019) Harmonisation of stem volume estimates in European NFIs. *Annals of Forest Science* 76, 23 p. <https://doi.org/10.1007/s13595-019-0800-8>
- GSFC Germany, 2019. *Ausblick: Shared Socioeconomic Pathways (SSPs) – Narrative für Szenariender nächsten Generation*. TCFD Think Tank. Available at: [https://gsfc-germany.com/wp-content/uploads/2019/08/190816\\_TCFD\\_socioeconomicpathways\\_DE.pdf](https://gsfc-germany.com/wp-content/uploads/2019/08/190816_TCFD_socioeconomicpathways_DE.pdf)
- Forzieri G., Girardello M., Ceccherini G., Spinoni J., Feyen L., Hartmann H., Beck P.S.A., Camps-Valls G., Chirici G., Mauri A., Cescatti A., 2021. Emergent vulnerability to climate-driven disturbances in European forests. *Nature Communications*. Available at: <https://doi.org/10.1038/s41467-021-21399-7>
- Haslinger, K., Schöner, W., Anders, I. (2016). Future drought probabilities in the Greater Alpine Region based on COSMO-CLM experiments – spatial patterns and driving forces. *Meteorologische Zeitschrift*, 25, 137-148.
- Haslinger, Klaus & Hofstätter, Michael & Kroisleitner, C. & Schöner, Wolfgang & Laaha, Gregor & Holawe, Franz & Blöschl, G.. (2019). Disentangling Drivers of Meteorological Droughts in the European Greater Alpine Region During the Last Two Centuries. *Journal of Geophysical Research: Atmospheres*. 124. 10.1029/2018JD029527.
- Ledermann T., Jandl R., Veselinovic B., Hager H., Diwold G., Hochbichler E., Sommerauer M. , 2010: Ein Ansatz zur Abschätzung der sturminduzierten Ausfallwahrscheinlichkeit von Fichten- und Buchenbeständen des öster-reichischen Alpenvorlandes. In: *Forstwissenschaften: Grundlage nachhaltiger Waldbewirtschaftung*. Beiträge zur Forstwissenschaftlichen Tagung 2010 in Göttingen, Cuvillier Verlag: S. 61
- Matulla, C., W. Schoener, H. Alexandersson, H. von Storch, and X.L. Wang, 2008: European storminess: late nineteenth century to present. *Climate Dynamics*, 31(2-3), 125-130.
- Mauri, A. et al. 2017. EU-Forest, a high-resolution tree occurrence dataset for Europe. – *Sci. Data* 4: 160123.
- Pasztor F, Matulla C, Rammer W, Lexer MJ (2014) Drivers of the bark beetle disturbance regime in Alpine forests in Austria. *For Ecol Manage* 318:349–358. doi:10.1016/j.foreco.2014.01.044

- Pasztor F, Matulla C, Zuvella-Aloise M, Rammer W, Lexer MJ. Developing predictive models of wind damage in Austrian forests. *Annals of Forest Science*. 2015;72:289–301.
- Riahi, K., Vuuren, D.P. van, Kriegler, E., Edmonds, J., O'Neill, B.C., Fujimori, S., Bauer, N., Calvin, K., Dellink, R., Fricko, O., Lutz, W., Popp, A., Cuaresma, J.C., KC, S., Leimbach, M., Jiang, L., Kram, T., Rao, S., Emmerling, J., Ebi, K., Hasegawa, T., Havlik, P., Humpenöder, F., Silva, L.A.D., Smith, S., Stehfest, E., Bosetti, V., Eom, J., Gernaat, D., Masui, T., Rogelj, J., Strefler, J., Drouet, L., Krey, V., Luderer, G., Harmsen, M., Takahashi, K., Baumstark, L., Doelman, J.C., Kainuma, M., Klimont, Z., Marangoni, G., Lotze-Campen, H., Obersteiner, M., Tabeau, A. and Tavoni, M., 2017. The shared socioeconomic pathways and their energy, land use, and greenhouse gas emissions implications: An overview. *Global environmental change*, 42, pp.153–168. Available at: <https://doi.org/10.1016/j.gloenvcha.2016.05.009>
- Santoro M., 2018. GlobBiomass—global datasets of forest biomass.
- Schueler, S. et al. 2014. Vulnerability of dynamic genetic conservation units of forest trees in Europe to climate change. – *Global Change Biol*. 20: 1498–511.
- Vauhkonen J., Berger A., Gschwantner T., Schadauer K., Lejeune P., Perin J., u.a. , 2019: Harmonised projections of future forest resources in Europe. *Annals of Forest Science*, Cham, 76(3): Article 79:
- Verkerk, P.J., Levers, Ch., Kuemmerle, T., Lindner, M., Valbuena, R., a, Verburg, P.H., Zudin, S., 2015. Mapping wood production in European forests. *Forest Ecology and Management* 357 (2015) 228–238.
- Vuuren, D.P. van, Edmonds, J., Kainuma, M., Riahi, K., Thomson, A., Hibbard, K., Hurtt, G.C., Kram, T., Krey, V., Lamarque, J.F., Masui, T., Meinshausen, M., Nakicenovic, N., Smith, S.J. and Rose, S.K., 2011. The representative concentration pathways: an overview. *Climatic Change*, 109(1-2), pp.5–31. Available at: <https://doi.org/10.1007/s10584-011-0148-z>